AD NUMBER

AD860705

LIMITATION CHANGES

TO:

Approved for public release; distribution is unlimited.

FROM:

Distribution authorized to U.S. Gov't. agencies only; Administrative/Operational Use; OCT 1969. Other requests shall be referred to Space and Missile Systems Organization, Los Angeles, CA 90045.

AUTHORITY

SAMSO ltr, 116 Aug 1973

AEDC-TR-69-175

EFFECTS AND CONTROL OF CONTAMINATION FROM A SCALED MOL ATTITUDE CONTROL THRUSTER IN A RADIAL ORIENTATION

David W. Hill, Jr. and Dale K. Smith
ARO, Inc.

October 1969

AEROSPACE ENVIRONMENTAL FACILITY
ARNOLD ENGINEERING DEVELOPMENT CENTER
AIR FORCE SYSTEMS COMMAND
ARNOLD AIR FORCE STATION, TENNESSEE

NOTICES

When U. S. Government drawings specifications, or other data are used for any purpose other than a definitely related Government procurement operation, the Government thereby incurs no responsibility nor any obligation whatsoever, and the fact that the Government may have formulated, furnished, or in any way supplied the said drawings, specifications, or other data, is not to be regarded by implication or otherwise, or in any manner licensing the holder or any other person or corporation, or conveying any rights or permission to manufacture, use, or sell any patented invention that may in any way be related thereto.

Qualified users may obtain copies of this report from the Defense Documentation Center.

References to named commercial products in this report are not to be considered in any sense as an endorsement of the product by the United States Air Force or the Government.

EFFECTS AND CONTROL OF CONTAMINATION FROM A SCALED MOL ATTITUDE CONTROL THRUSTER IN A RADIAL ORIENTATION

David W. Hill, Jr. and Dale K. Smith
ARO, Inc.

FOREWORD

The work reported herein was performed at the request of Space and Missile Systems Organization (SAMSO), Air Force Systems Command (AFSC), under Program Element 35121F, Program Area 632A.

The rocket engine and simulated vehicle skin were designed and fabricated by Marquardt Corporation and McDonnell Douglas Corporation, Missiles and Space Systems Division (MSSD), respectively.

The test results were obtained by ARO, Inc. (a subsidiary of Sverdrup & Parcel and Associates, Inc.), contract operator of the Arnold Engineering Development Center (AEDC), AFSC, Arnold Air Force Station, Tennessee, under Contract F40600-69-C-0001. The tests were conducted from May through December 21, 1968, under ARO Project No. SB0721, and the manuscript was submitted for publication on July 10, 1969.

Information in this report is embargoed under the Department of State International Traffic in Arms Regulations. This report may be released to foreign governments by departments or agencies of the U.S. Government subject to approval of the MOL Project Office (SAFSL-5B), or higher authority within the Department of the Air Force. Private individuals or firms require a Department of State export license.

This technical report has been reviewed and is approved.

Robert T. Otto
Major, USAF
AF Representative, AEF
Directorate of Test

Roy R. Croy, Jr.
Colonel, USAF
Director of Test

ABSTRACT

A test was conducted to determine the effects of contamination produced by a 1-lb scaled Manned Orbital Laboratory thruster. The test required pulsing the 1-lb attitude control thruster in its radial orientation and determining the effects of contaminates from the thruster impinging on optical and thermal control surface test specimens located on a flat plate exposed to the thruster exhaust plume. The thruster was pulsed with durations of 20, 50, 100, and 1000 msec with 1000 msec off time at altitudes above 400,000 ft. Significant contamination was produced for the pulse-mode operation. Methods for control of contamination from the thruster and on the plate were investigated. In situ reflectance, emittance, and transmittance measurements were made on the optical and thermal control surface test specimens under vacuum conditions and at atmospheric pressure. Pretest and posttest laboratory measurements were made at atmospheric conditions. Contamination deposited on the plate was near and below the thruster exit, and the amount of contamination produced by the thruster decreased as the thruster pulse duration increased. Contamination controls evaluated during the test were the heated shroud and a fence located on the plate. The heated shroud was effective in reducing contamination on the plate; however, it did not eliminate the contaminates produced by the thruster in the plume. The in situ reflectance and transmittance measurements made on the specimens at the simulated altitude were more realistic of the contamination encountered by the specimens from the thruster exhaust than the atmospherical posttest laboratory measurements.

CONTENTS

APPENDIXES

Figure Page

NOMENCLATURE

h	Distance from center of nozzle exit plane to the plate
J	Solar spectral irradiance as defined by Johnson
P_c	Combustion chamber pressure, psia
P_F	Fuel inlet pressure, psia
P_{ox}	Oxidizer inlet pressure, psia
R	Spectral reflectance
$\bar{R}$	Average visible reflectance
S	Calibration factor

T	Spectral transmittance
$\bar{T}$	Average visible transmittance
Tem	Temperature of emissometer
T_o	Initial prefire spectrum
T_s	Temperature of specimen
t_s	Relative solar transmittance
Vem	Voltage of emissometer
x	Distance from thruster exit plane
y	Transverse distance from thruster axis
z	Distance from detector to surface of panel
α	Angle between thruster axis and surface of plate, deg
α_s	Solar absorptance
ϵ	Emittance
θ	Angle of instrument rotation
μ	Wavelength, microns
ν	Wave number, cm^{-1}

SECTION I
INTRODUCTION

The exhaust plumes from attitude control rocket engines fired at orbital attitudes expand to the extent that the exhaust products strike spacecraft surfaces and externally mounted components located within a large envelope extending downstream from the nozzle exit plane. The impingement of the gas results in local surface heating, surface pressures, and possible contamination of spacecraft surfaces. These effects may cause malfunctions of apparatus mounted on or inside the spacecraft. It is, therefore, important to identify and understand the conditions that cause these effects so that they may be properly considered in the design and operation of the spacecraft. There have been several analytical predictions of exhaust plume behavior (Refs. 1 and 5) and some limited experimental tests at high altitude (Refs. 1 through 5). These tests have been limited to short durations with transient altitudes from 400,000 to 200,000 ft.

A series of tests was conducted at AEDC in a 10-ft-diam chamber to determine plume symmetry (Ref. 6); heat flux and surface pressures (Ref. 7); and effects of contamination (Refs. 8 and 9) from a 1-lb thruster plume impinging on flat plates at altitudes over 400,000 ft. The 1-lb thruster is scaled to simulate both the 100-lb (longitudinal orientation) translational thruster, and the 22-lb (tangential and radial orientation) attitude control thrusters of the Manned Orbital Laboratory (MOL) as shown in Fig. 1, Appendix I. The flat plate simulates the MOL surface. The purpose of this test was to determine if contamination is produced by the 1-lb scaled attitude control thruster in its radial orientation, to identify any contaminate produced, and to determine the performance degradation, if any, of optical and thermal control surfaces that have been exposed to contamination. The test required that the 1-lb scaled thruster be fired in pulses with pulse durations from 20 to 1000 milliseconds (msec) while maintaining a minimum simulated altitude of 400,000 ft.

SECTION II
TEST FACILITY

The test was conducted in the Aerospace Research Chamber (ARC) (8V) of the Aerospace Environmental Facility. The stainless steel chamber (Fig. 2) is 20 ft long and 10 ft in diameter. The cryopumping surfaces were designed (Ref. 10) for removing gas products from rocket engines and low density nozzles of high enthalpy. The 620 ft^2 of liquid-nitrogen (LN_2)-cooled surfaces, 800 ft^2 of gaseous-helium (GHe)-cooled surfaces, and 50 ft^2 of liquid-helium (LHe)-cooled surfaces were arranged to remove 16 kw from the exhaust gas products in an optimum manner.

The sketch below and Fig. 2 show the arrangement of the cryosurfaces to pump the high enthalpy exhaust gas products. The gas leaving the engine passes through the radially arranged, forward GHe surfaces and impinges on the annular LN_2 cryosurface where 8 kw is removed. The cooled gas is then either cryopumped by the LN_2 surface or reflected onto the GHe cryosurface where it is condensed. There is a total GHe refrigeration capacity of 8 kw–7 kw for the front GHe cryopump and the remaining 1 kw for the rear section. Since hydrogen (H_2) has a high vapor pressure (10^{-4} torr) on 15°K GHe surfaces, LHe (4.2°K) was used to remove the H_2 in the plume. The H_2 and

nitrogen (N_2) exhaust gases moving axially down the chamber impinge on the LN_2 precooler, where energy is removed, and then are cryopumped on the LHe cryosurfaces.

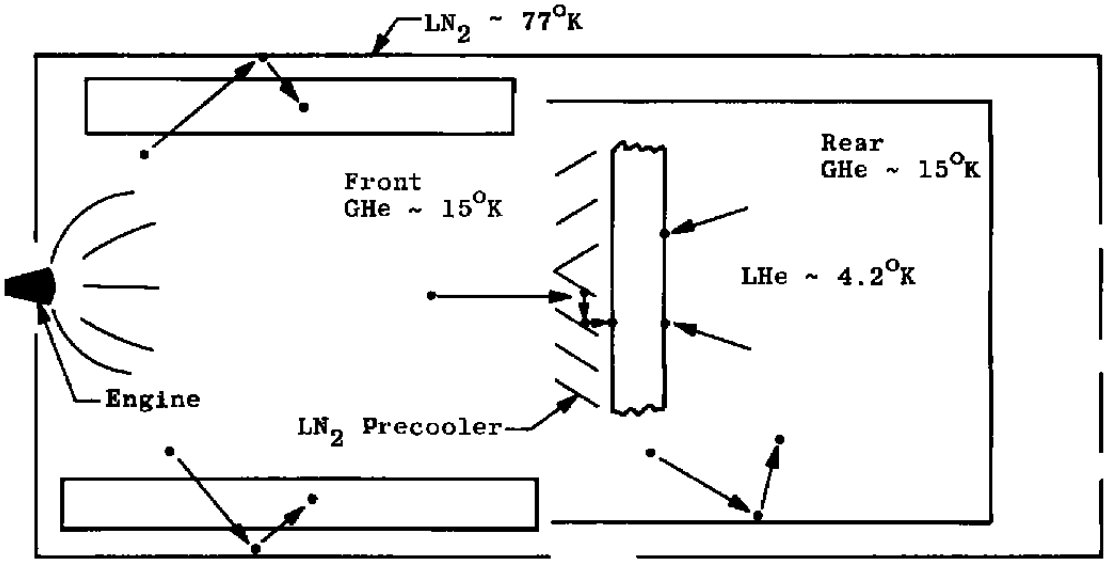

The front GHe cryosurfaces consist of fifty-two 8- by 1-ft panels positioned in a radial array about the axis of the chamber. The rear GHe cryosurface is 8 ft long and 6 ft in diameter. The supply of the gas to the front or rear GHe cryosurfaces could be distributed by externally operated valves.

The LHe was made in the Aerospace Environmental Facility. A 30-liter/hr He liquefier was used in conjunction with a 4-kw GHe refrigerator as a precooler for the gas. A 1000-liter dewar located on top of the chamber housed a Joule-Thompson valve for the final stages of liquefaction and stored the LHe.

SECTION III
TEST ARTICLES

3.1 1-LB-THRUST SCALED THRUSTER

The 1-lb-thrust MOL scaled thruster used in the test was supplied by Marquardt Corporation. The bipropellant, monomethylhydrazine and nitrogen tetroxide ($MMH\text{-}N_2O_4$) thruster (Fig. 3) was designed for both steady and pulsing operation. The performance of the engine was investigated by Marquardt Corporation personnel who found that the lower thrust level with pulsing performance resulted in lower combustion efficiency. During the firing, the propellant valves and injectors were held at 60°F with cooling water.

The thruster design parameters and performance are shown below.

Thrust	1.0 lb
Fuel	MMH (Monomethylhydrazine)
Oxidizer	N_2O_4
Chamber Pressure	90 psi
Mixture Ratio	1.65 ± 1.5
Nozzle Expansion Ratio	40:1
Nozzle Geometry	Contoured
Chamber Temperature	4000°F
Throat Diameter	0.090 in.
Nozzle Exit Diameter	0.569 in.
Combustion Efficiency	0.830

Shown in Fig. 3 is the assembled 1-lb thruster. It consists of a water-cooled, single-doublet injector head, two fast response solenoid valves, and two 5-micron (μ) nominal filters upstream of each valve. The nozzle and combustion chamber are an integral part, machined from molybdenum.

Figure 4 shows the 1-lb thruster propellant system. The system consists mainly of three parts: the engine N_2 purge, high-point bleeds, and propellant supply system. Each propellant tank has a capacity of 2 liters. The propellants were pressurized with dry N_2. The propellant lines were 0.180-in.-ID stainless steel tubing.

3.2 TEST PANEL

The test panel (Fig. 5) used during the radial thruster orientation test was 22.5 in. wide by 34 in. long. The panel was mounted, as shown in the top view of Fig. 6, on a pivot point so it could be rotated remotely from a position for measuring which was parallel to the ARC 8V chamber centerline to a position for thruster firing which was perpendicular to the chamber centerline. The thruster was mounted in a fixed position perpendicular to the panel with the nozzle exit plane 0.70 in. from the surface of the panel. Figure 7 is a photograph of the test panel and thruster in the measuring position.

There are twenty-eight 1-in.-diam holes and six 1.5-in.-diam holes drilled through the panel for the purpose of inserting specimens (Fig. 5).

3.3 SPECIMENS

Eight types of specimens were used during the test to simulate the thermal control coatings and optical surfaces on the outside of the MOL vehicle. They are the following:

Type	Description	Use on MOL Vehicle
A	Zine Oxide and Potassium Silicate ($ZNO + K_2 SiO_3$)	Radiator Coating
D	Polished Aluminum	Thermal Control

Type	Description	Use on MOL Vehicle
G	Fused Quartz (High Efficiency Anti-reflective Coating)	View Port Window
H	Germanium Glass/Fluoride Coating	Horizon Sensor Window
K	Black Spinal (Potassium Silicate)	Laboratory Module Coating
M	High Quality Mirror (Optical Grade)	Startracker
W	Quartz (Optical Grade)	Window
VVSA	Teflon®	Velocity Vector Sensor Assembly (VVSA)

The above thermal control and optical specimens were each applied or attached to a 15/16-in.-diam disk which was mounted on a specimen holder (Fig. 8). The holder was threaded so it could be inserted into holes of the test panels (Fig. 5). The holders contained a heater tape with a thermocouple for maintaining the specimens at 60°F while in the vacuum. The velocity vector sensor assembly was mounted in location S_1 (see Fig. II-1, Appendix II) and was approximately 4 in. from the thruster and 1.5 in. above the panel surface.

3.4 THRUSTER SHROUD

Figure 9 illustrates the shroud used during the tests in an attempt to reduce the contamination on the test panels by capturing and decomposing the contaminants dripping from the nozzle exit. The shroud was provided with two electrodes for electrical heating.

SECTION IV
TEST INSTRUMENTATION

4.1 THRUSTER INSTRUMENTATION

The thruster was instrumented with three Taber® 500-psia pressure transducers. Two were used on the inlet side of the injector head for monitoring oxidizer and fuel pressures. One transducer was located on the engine combustion chamber. The response time of the transducers is less than 1 sec.

4.2 CHAMBER INSTRUMENTATION

There were four Bayard-Alpert-type ionization pressure gages located at various positions in the chamber. One gage was located behind the thruster for measuring the pressure during firings. The remaining gages were positioned near the LHe cryopump in order to evaluate its performance. One Alphatron® and one Baratron® were installed behind the thruster for monitoring pressures above 10^{-3} torr.

4.3 SCANNER MECHANISM

A scanner mechanism was installed in the test chamber (Fig. 6) to mount and position instrumentation for in situ measurements. The scanner mechanism provided the instruments four degrees of movement: three linear - x. y and z; and one angular - θ. Each movement was driven by a gear train and motor which could be controlled from outside the chamber. A light source was placed behind and adjacent to each specimen, transmitting a light beam through an appropriately located small hole in the panel. A photocell was mounted on each of the in situ measuring instruments. When the instrument was properly positioned relative to the desired specimen, the light beam impinged on the photocell and gave positive indication that the test instrument on the scanner mechanism was correctly located for the measurement.

4.4 IN SITU MEASUREMENTS

A Block Engineering, Inc. Model P-4 interferometer spectrometer and a locally fabricated emissometer (Ref. 11) were mounted on the scanner mechanism for making in situ measurements. The P-4 spectrometer was equipped with a locally designed and fabricated integrating sphere attachment (Ref. 11). The P-4 instrument is a quartz-polarization interferometer spectrometer which measures spectra in the range of 4,000 to 27,000 cm^{-1} (0.27 to 2.5 μ). The P-4 was used to measure in situ absolute spectral reflectance, $R(\nu)$, for the thermal control surface and mirror specimens, and relative spectra, $T(\nu)$, of the light transmitted through the window specimens from a tungsten lamp. The emissometer was used for making in situ total emittance, ϵ, measurements on selected thermal control surface specimens during the test. The raw data were reduced for analysis and presentation as described in Section 5.2.

4.5 LABORATORY MEASUREMENTS

The spectral reflectance of the specimens before and after each test were measured with a Beckman DK-2A spectroreflectometer in the 0.25- to 2.5-μ wavelength region. The instrument has been modified (Ref. 12) to measure absolute, directional-hemispherical spectral reflectance. For the present tests, the instrument was installed and operated in an airtight box which was purged with dry N_2. All postfire measurements were taken before the samples were exposed to air.

4.6 DATA SYSTEM

Figure 10 shows a schematic of the test data system which was used during the test. The specimen temperatures, P-4 spectrometer signals, emissometer, and engine flow

rate data went into signal conditioning equipment, a commutator, analog-to-digital converter, digital tape, and then to the computer and/or data printout. In addition, for rapid analysis, the engine pressures and flow rates were recorded directly on an oscillograph.

SECTION V
PROCEDURE

5.1 TEST PROCEDURE

Before and after each test, DK-2A reflectance measurements were made on selected test specimens in the laboratory. White gloves were used in handling the specimens. After completing installation of specimens in the test panels, the proper scanner mechanism movement at each specimen location was checked by remote operation using position indicators (x, y, z, and θ) located outside the chamber.

After the thruster position was set, the chamber was purged with N_2 and then evacuated, first by means of a 140-cfm mechanical pump, and then by a 6-in. diffusion pump. These pumps evacuated the chamber to 10^{-4} torr pressure. At this time, the LN_2 and GHe liners were cooled down. With the cryosystems at the desired temperatures, the chamber pressure stabilized at approximately 10^{-7} torr. In situ reflectance, transmittance, and emittance measurements were then taken on selected specimens. After completing the measurements, the scanner mechanism was moved to the parking position for firing (Fig. 6). The propellant tanks and lines were then pressurized, the test panel was rotated to its firing position (Fig. 6), and the LHe cryopump was cooled down to 4.2°K. After a selected number of firings, in situ measurements were repeated on the specimens with the panel in the measuring position. After completion of the firings, the chamber was pressurized to atmosphere with dry N_2 where, in some cases, sea-level in situ measurements were repeated on the specimens.

In order to prevent exposure of the specimens to air, following the test, personnel entered the dry N_2 atmosphere chamber with special breathing apparatus and placed the specimens in special containers for transmittal to the laboratory.

5.2 DATA REDUCTION

Laboratory measurements of absolute spectral reflectance and transmittance resulted in continuous curves drawn by an x-y plotter as the measurement was made at each wavelength.

In situ measurements for spectral reflectance and transmittance also resulted in plots by an x-y plotter, but the curves were not continuous and were not drawn as the measurement was made. Data reduction for the in situ spectrometer was done by a computer which produced a series of discrete values from which the curves were plotted. These discrete values were stored in computer memory before plotting and hence were available for further computation.

The absolute spectral reflectance data, $R(\nu)$, for the mirror and thermal control surface specimens were reduced by computer to obtain the average visible reflectance, $\overline{R}$, which is defined by

$$\overline{R} = \frac{\int_{12,500}^{27,000} R(\nu)\, d\nu}{\int_{12,500}^{27,000} d\nu}$$

The absolute spectral reflectance curves are included in the figures of Appendix I, and the corresponding computed values for the average visible reflectance, $\overline{R}$, are included in the data tabulated in Appendix III.

The absolute spectral reflectance data, $\overline{R}(\nu)$, were also used to compute values for the solar absorptance, a_s, in accord with

$$a_s = \frac{\int_{4,000}^{27,000} [1 - R(\nu)]\, J(\nu)\, d\nu}{\int_{4,000}^{27,000} J(\nu)\, d\nu}$$

where $J(\nu)$ is the generally accepted Johnson solar spectral irradiance. The values of a_s calculated for the mirror and thermal control surface samples are included in the data tabulated in Appendix III.

Spectral curves of the transmittance lamp, modified by the transmittance of the window specimen and attenuation in the spectrometer, which were obtained during testing, were used with initial, pretest spectra to compute the relative spectral transmittance, T/T_o (υ), which is plotted in the figures of Appendix I. These values were used, in turn, to compute values of average visible relative transmittance, $\overline{T}$, defined by

$$\overline{T} = \frac{\int_{12,500}^{27,000} [T/T_o(\nu)]\, d\nu}{\int_{12,500}^{27,000} d\nu}$$

The computed values of $\overline{T}$ are tabulated in Appendix III with the other reduced data.

The relative spectral transmittance was also used to compute the relative solar transmittance, t_s, which is defined by

$$t_s = \frac{\int_{4,000}^{27,000} [T/T_o(\nu)]\, J(\nu)\, d\nu}{\int_{4,000}^{27,000} J(\nu)\, d\nu}$$

where, again, $J(\nu)$ is the Johnson solar spectral irradiance. The values of t_s are also tabulated in Appendix III.

In situ measurements of emittance for the thermal control surface specimens resulted in a value, ϵ, calculated from the emissometer voltage, Vem, the specimen temperature, T_s, and the emissometer temperature, Tem, in accord with

$$\epsilon = \frac{Vem}{(T_s^4 - Tem^4)S}$$

where S is a calibration factor. Values of ϵ are also tabulated in Appendix III.

In addition to the preceding values which were calculated directly from measured data, the ratio α_s/ϵ was computed for the thermal control surface specimens; and values of the ratio are included with the other data tabulated in Appendix III.

SECTION VI
DISCUSSION AND RESULTS

The effects of rocket exhaust plume impingement on surface coatings in the contamination tests conducted can be categorized into the following (Refs. 8, 9, and 13):

a. Erosion or ablation of the coatings as a result of aerodynamic heating.

b. Chemical corrosion of the coatings as a result of unburned propellants reacting with the coatings.

c. Condensation or deposition on the coatings.

In the present tests (radial orientation), the aerodynamic heating effect is insignificant because of the short duration of firing (1000 msec or less) as compared to 1000 msec off time, and the amount of exhaust gases impinging on the panel is small because the thruster was firing away from the test panel. For this thruster orientation and duty cycle. the maximum observed temperature on the panel was 75°F. Most surface coatings are designed to withstand temperatures greater than 75°F. The heating effect is more evident in the steady-state thruster operation (greater than 1000 msec) where the maximum observed temperature on the panel is 650°F (Ref. 7). Chemical corrosion occurs when the unburned propellants deposited on the surface coatings react with the coatings and create permanent damage. Since the rocket exhaust plume composition is approximately 30-percent water vapor by weight (Ref. 13), condensation is more likely to occur on the low temperature coatings. This condensation would be temporary contamination since it would evaporate with higher operational surface temperatures.

Since the contamination tests of the longitudinal, radial, and tangential orientations were not conducted in sequence, the test numbers reported for this phase (radial orientation) will not be consecutive. There were a total of three tests with the thruster angle fixed at 90 deg and 0.70 in. from the surface of the test panel (see Fig. 6). Within each test, the objective, results, test hardware, measurements, and number of firings varied as indicated in Appendixes II and III.

The thruster was fired with pulse durations of 20, 50, 100, and 1000 msec with 1000-msec off time between pulses. Figure 11 shows a plot of combustion chamber pressure as a function of pulse firing time. From the figure it can be seen that the combustion chamber pressure for 1000 msec approaches 90 psia, the design steady-state pressure.

Figure 12 shows the ARC 8V predicted chamber performance as a function of engine thrust level. From the figure it can be seen the 1-lb thruster can be fired indefinitely (more than 100 sec) maintaining 8 x 10^{-5} torr chamber pressure. For thruster pulsing, the ARC 8V chamber pressure would be lower than for steady-state firing as shown in Fig. 13. As can be seen from the figure, the altitude decreases from 600,000 to 400,000 ft for pulses from 20 to 1000 msec, respectively.

The full-scale 22- and 100-lb thrusters use multiple hole injectors for providing optimum combustion. The injector holes have to introduce and meter the flow to the combustion chamber and atomize and mix the propellants by impingement in such a manner that a correctly proportioned, homogenious fuel-oxidizer mixture will result, one that can be readily vaporized and burned. Only the nozzle of the 1-lb thruster and mass flow rate were scaled from the full-scale thrusters. The valves were the same as for the 22- and 100-lb engines. Because of the relatively small mass flow rate of the 1-lb scaled thruster, a single doublet injector design resulted (Fig. 3). In such a simple design, misalignment of either the oxidizer or fuel injector hole can result in incomplete combustion, especially in the pulse-mode operation. The accumulated unburned propellants in the combustion chamber would be blown out of the nozzle.

Another possibility for the formation of the unburned propellants in the combustion chamber is from the "dribble volume" located between the valve seat and the exit of the injector holes. When the valves are closed, the propellants within this volume flow into the combustion chamber; when the thruster is again fired, the residue is blown out of the combustion chamber into the nozzle. Therefore, more contamination would be expected in the pulse-mode than in the steady-state operation. In addition, since this engine had an abnormally large dribble volume to combustion chamber size, the likelihood of contamination formation is large.

Two methods of control were attempted in these tests to minimize the contamination deposited from the plume on the coatings: (1) A heated shroud was employed to collect and decompose the contamination at the exit of the thruster and (2) a shield or fence was used on the panel. Because of the large amount of contamination ejected from the thruster and the generally random distribution of contamination on the test panel, visual observations rather than optical measurements were used to evaluate the effectiveness of methods for controlling the contamination.

6.1 TEST 17

During test 17, large amounts of reddish-brown liquid contamination collected at the thruster exit momentarily and then were blown by the rocket exhaust onto the panel and coating samples. The appearance of this contamination occurred continuously after

the first 10 or 15 pulses (20- and 50-msec durations). A large quantity of contamination (approximately half a cup after 3000 pulses) impinged or dripped on the surface of the panel. The photograph in Fig. 7 shows this large buildup of contamination on the panel directly under the thruster (approximately 0.75-in. thick on the panel surface) during the test.

Reddish-brown contamination deposits were visible on specimens located at A_2, V_2, and H_2. This was caused from a gravity flow effect (see Fig. 7): the contamination that impinged on the panel in the vicinity of the thruster exit had flowed under the influence of gravity down the panel, thus contaminating every specimen in its path. Contamination deposits were also visible on the velocity vector sensor assembly. All other specimens showed little, if any, contamination after being exposed to the plume. This was expected since the thruster is firing directly out from the panel; therefore, these specimens were in the more rarefied regions of the plume.

Most of the specimens became contaminated when the chamber was repressurized to atmosphere. This was caused by the contamination on the cryosurfaces migrating through the chamber and to the test panel when the cryosurfaces became warn.

Figures 14 through 21 show the reflectance on specimens after being subjected to the environmental cycle. As can be seen from Figs. 14, 17, 18, 19, 20, and 21, the magnitude or trend of the data depend on the environment in which the measurements were made (i.e., in a vacuum or at atmosphere) as mentioned in Refs. 8 and 9. Therefore, the in situ measurements better represent the change in radiative properties of specimens because of exposure to the plume; and so most of the data presented in this report are for specimens on which in situ measurements were made.

Figures 22 and 23 show the change in transmittance on specimens located at S_{27} and V_2 after being exposed to the plume. Figure 22 also shows the reflectance on the window located at S_{27}. Measurement 3 on Fig. 23 was taken before the contamination reached location V_2 from the gravity flow effect.

6.2 TEST 18

In Test 18 a heated shroud and "container" with vacuum valve were used (Fig. II-1, Appendix II) to reduce contamination on the panel and to collect the contamination generated, respectively. The heated shroud proved effective in reducing the contamination on the panel and subsequent flow down the panel that was experienced in test 17, and it reduced somewhat the contamination on the VVSA specimen. However, the shroud did not eliminate the contaminates in the plume produced by the thruster.

Contamination still occurred on most of the specimens when the chamber was brought to atmosphere and was typical in all tests.

Figures 24 through 30 show the reflectance or transmittance measurements on the specimens before installation and after removal from the test panel. The trends were the same as for test 17 for pretest and posttest laboratory measurements.

6.3 TEST 19

In test 19, a heater shroud and collector flask were used for the same objectives as in test 18, and the results from visual observations were the same as for test 18.

Figures 32 through 42 show the change in reflectance on specimens after being exposed to the plume and environment. Figure 33 shows a large change in reflectance on specimen type A located at S_4 because of plume exposure (curves 2 and 3). The trends in radiative properties on the other specimens were the same as for tests 17 and 18.

6.4 SUMMARY

The thruster in the radial orientation was firing away from the panel; and, therefore, the amount of exhaust gases impinging on the panel and specimens was small. The velocity vector sensor assembly which was the closest specimen to the thruster and approximately 1.5 in. above the panel surface showed contamination deposition in test 17. Also in test 17 a large amount of contamination impinged or dripped on the panel near or below the thruster exit. The heated shroud proved to be an effective control in reducing the contamination on the test panel; however, it did not eliminate the contamination in the thruster plume.

Specimens which were alike showed approximately the same trends or magnitudes for all locations and tests for the thruster in radial orientation, and these trends were dictated by the environment in which the measurements were made. The following is a list of the maximum change in reflectance and the wavelength for which the maximum change occurred after being exposed to the plume for specimen types A and M.

Specimen Type	Location	Change in Reflectance, percent	Wavelength
A	S_4	38 - Decrease	0.72
M	S_{24}	9 - Decrease	0.40

Since the tests indicated that the contamination originated in the injector and combustion chamber of the 1-lb thruster, future test work should be conducted on various injectors to minimize the contamination. One possibility is to adapt the scaled nozzle to the full-scale injector and combustion chamber. The excess combustion gas, not required for thruster operation, could then be vented from the combustion chamber to outside the vacuum chamber.

SECTION VII
CONCLUSIONS

The results from the test for the control and effect of contamination ejected from a 1-lb scaled attitude control thruster in radial orientation is summarized by the following observations, conclusions, and recommendations:

1. The test indicated that a high degree of contamination resulted from the specific injector and combustion chamber configuration.

2. The amount of contaminates produced by the thruster decreased as the thruster pulse firing time increased (i.e., from 20 to 1000 msec).

3. The chemical analysis of the reddish-brown contamination collected during the tests indicated the contamination by weight was MMH (30.5 percent), H_2O (31.7 percent), and $-NO_3$ (37.8 percent).

4. Most of the contamination on the panel occurred near or below the thruster exit.

5. Specimen type A showed as much as an 38-percent decrease in reflectance. Other specimens exposed to the plume showed 10 percent or less change in reflectance.

6. The reflectance and transmittance measurements illustrate that the measurement environment (i.e., measurements in vacuum or atmosphere) affected the magnitudes or trends of the measurements made. The in situ measurements at the simulated altitudes are believed to be more representative of the true contamination on the panel than are the laboratory measurements.

7. The accumulation of contaminants at the thruster exit followed by ejection to the panel was eliminated by a heated shroud. However, it did not eliminate the contaminates in the plume produced by the thruster.

8. Further tests should be conducted to determine the variation in contamination production with varied injector and combustion chamber configurations.

REFERENCES

1. Llinas, J., Sheeran, J., and Hendershot, K.C. "A Short Duration Experimental Technique for Investigating Solid Propellant Rocket Plume Impingement Effects At High Altitudes." Cornell Aeronautical Laboratory, Buffalo, New York, ICRPG/AIAA 3rd Solid Propulsion Conference, No. 68-517, June 4-6, 1968.

2. Bauer, R.C. and Schlumpf, R.L. "Experimental Investigation of Free Jet Impingement on a Flat Plate." AEDC-TN-60-223 (AD253229), March 1961.

3. Barebo, R.L. and Ansley, R.C. "Effects of Rocket Exhaust Jet Impingement on a Movable Flat Plate at Pressure Altitudes above 200,000 Feet." AEDC-TDR-63-214, January 1964.

4. Llinas, J. "Electron Beam Measurements of Temperature and Density in the Base Region of a Clustered Rocket Model." Cornell Aeronautical Laboratory, Buffalo, New York, AIAA 2nd Flight Test Simulation and Support Conference, No. 68-236, March 25-27, 1968.

5. Burch, B.A. "Effect of Contamination on Spacecraft Surfaces Exposed to Rocket Exhausts," AEDC-TR-68-23 (AD831624L), April 1968.

6. Hill, D.W., Jr. "Investigation at High Altitudes of Rocket Exhaust Plume Symmetry and Interaction with a Plate with a Scaled MOL Thruster." AEDC-TR-69-75, April 1969.

7. Hill, D.W., Jr. and Smith, D.K. "Heat Flux and Pressure Measurements in an MOL Scaled Thruster Plume at 400,000-ft Altitude." AEDC-TR-69-84, May 1969.

8. Hill, D.W., Jr. and Smith, D.K. "Effects and Control of Contamination from a Scaled MOL Attitude Control Thruster in a Tangential Orientation." AEDC-TR-69-146, to be published.

9. Hill, D.W., Jr. and Smith, D.K. "Effects and Control of Contamination from a Scaled MOL Translational Thruster in a Longitudinal Orientation." AEDC-TR-69-152, to be published.

10. Heald, J.H., Jr., Dawbarn, R., and Arnold, F. "Test Chamber Concept Development for Very High Altitude Rocket Plume and Space Vehicle Systems Testing." AEDC-TR-68-205 (AD841628), October 1968.

11. Frazine, D.F. and Cox, G.S. "Instrumentation for Evaluating Effects of Plume Contamination on Optical Properties of MOL Spacecraft Surfaces," AEDC-TR-69-188, to be published.

12. Cox, George S. "Absolute Reflectance Measurements with a Ratio Recording Spectroreflectometer." AEDC-TR-69-123, to be published.

13. Borson, E.N. and Landsbaum, E.M. "A Review of Available Rocket Contamination Results." Aerospace Report No. TR-0200 (4250-20)-2.

APPENDIXES

I. ILLUSTRATIONS
II. TEST LOG
III. TABLES OF OPTICAL MEASUREMENTS

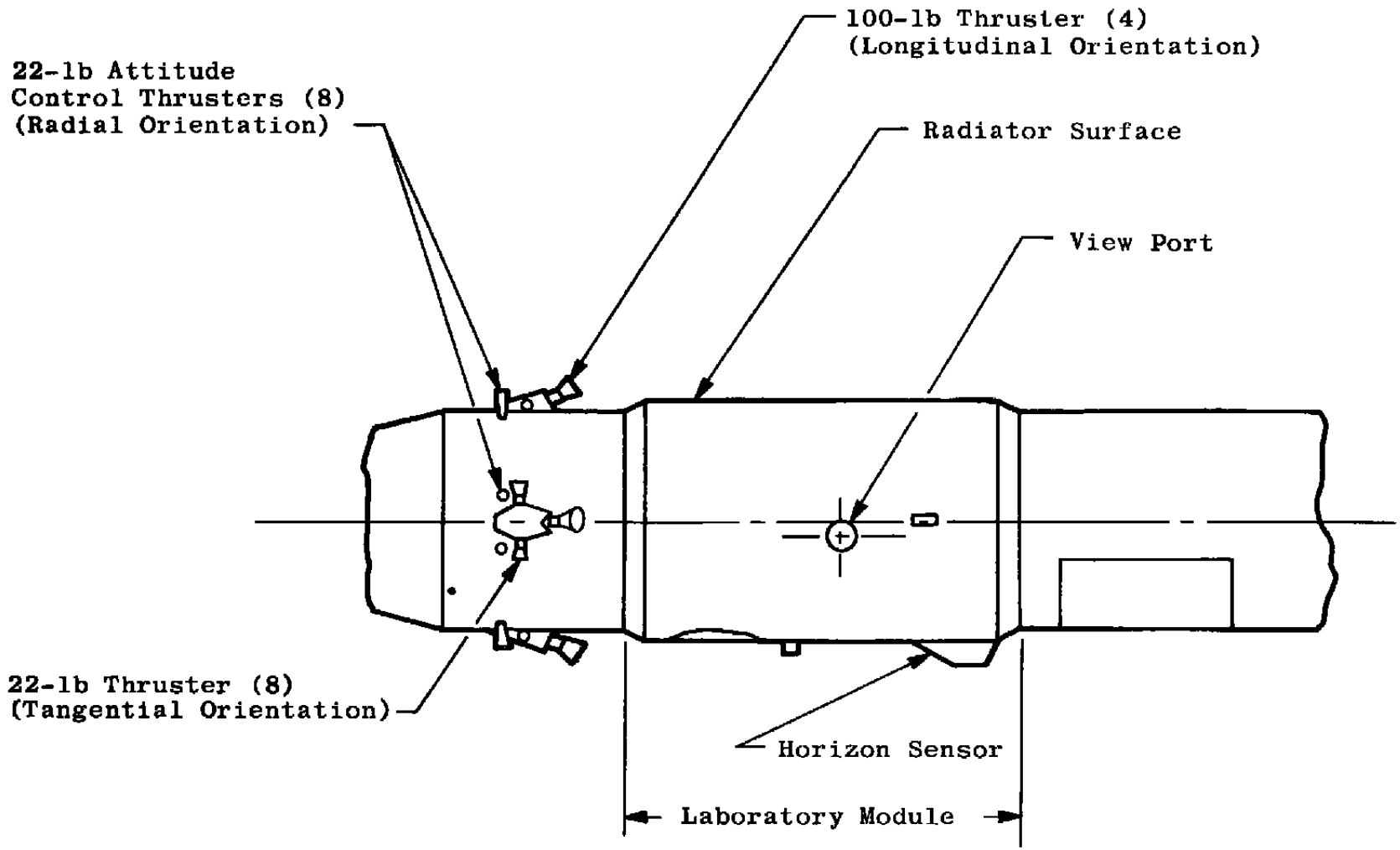

Fig. 1 Manned Orbital Laboratory with Thrusters

AEDC-TR-69-175

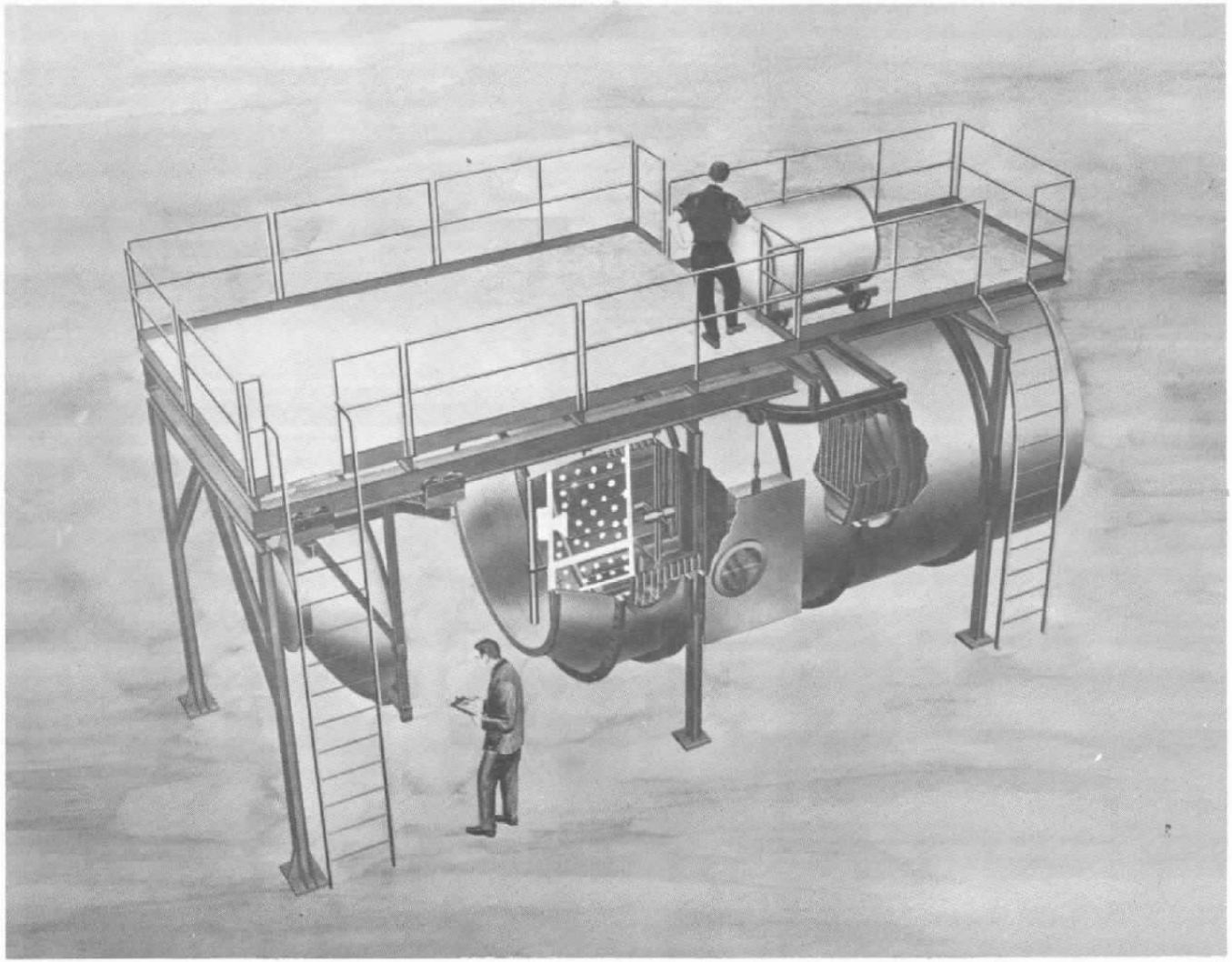

Fig. 2 Aerospace Research Chamber (ARC) (8V)

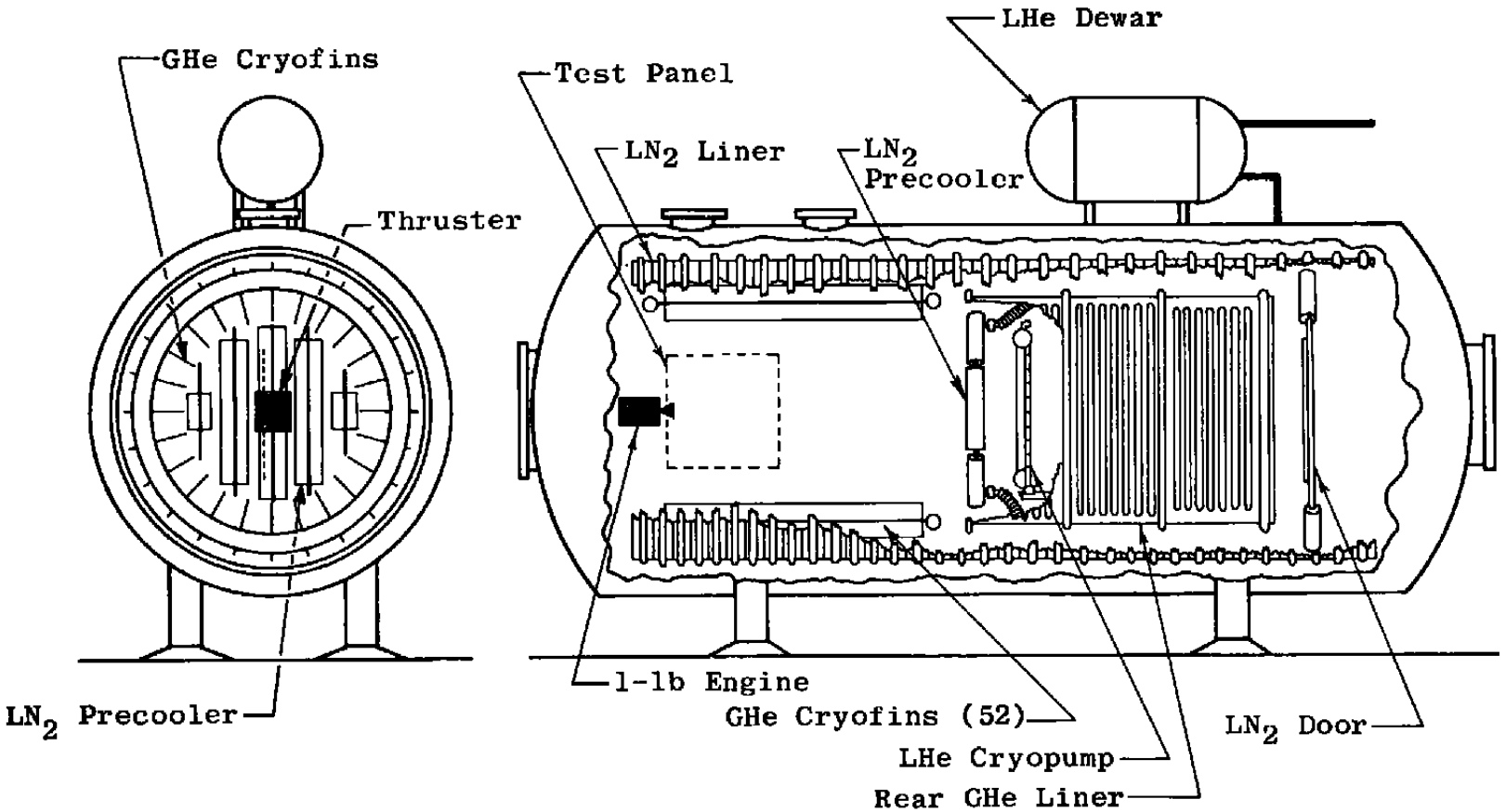

Fig. 2 Concluded

AEDC-TR-69-175

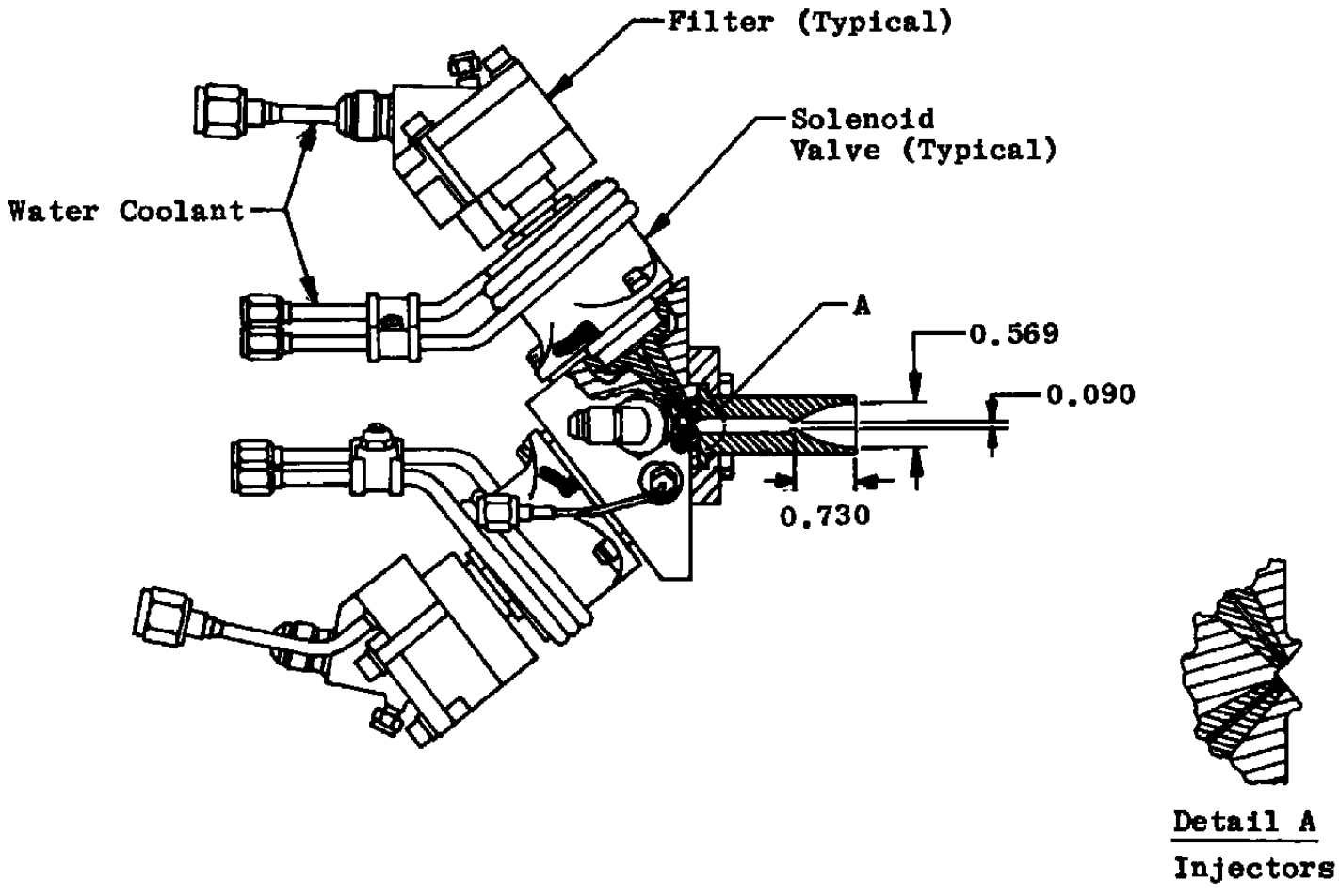

Fig. 3 1-lb-Thrust Engine and Components

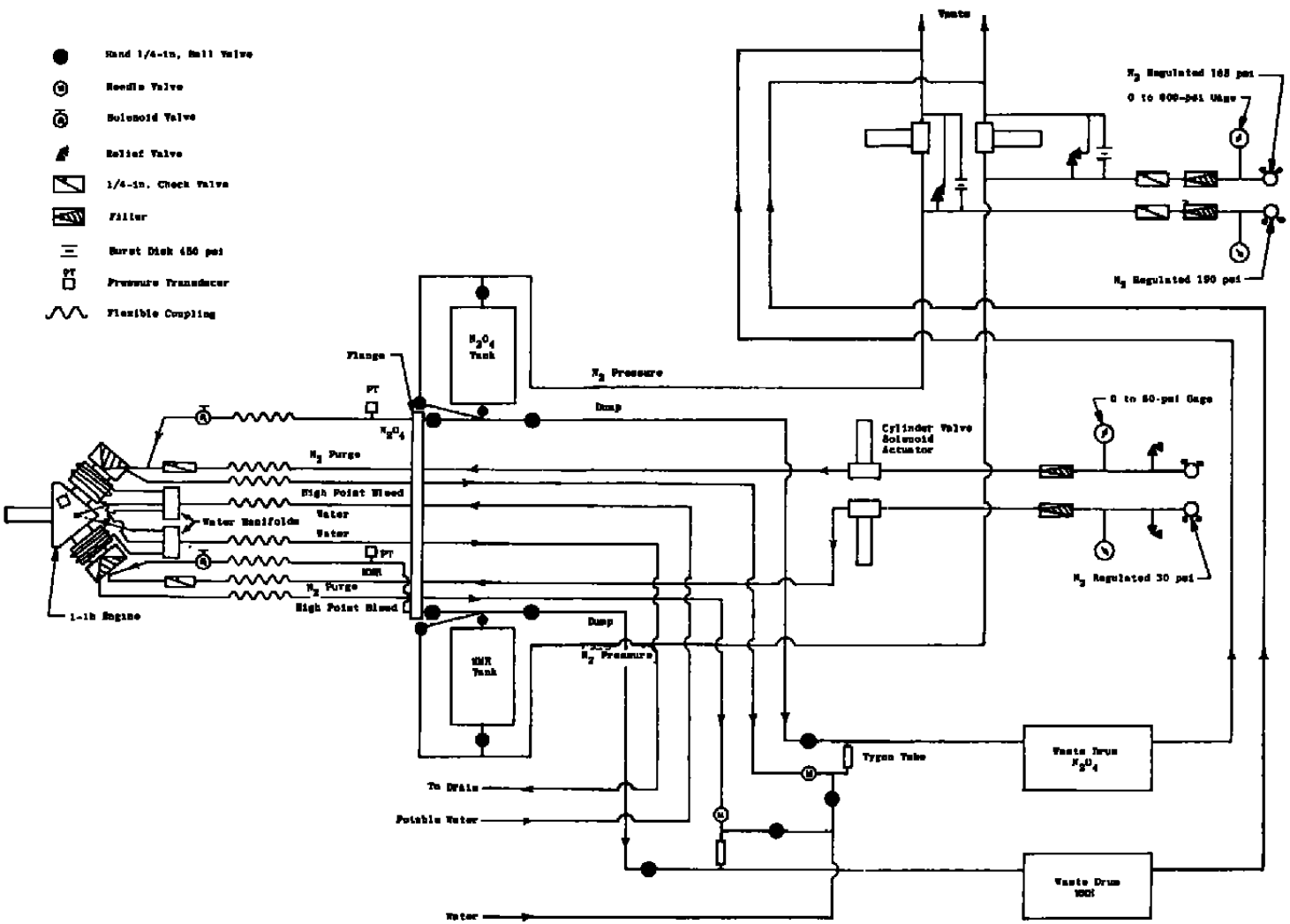

Fig. 4 Propellant System

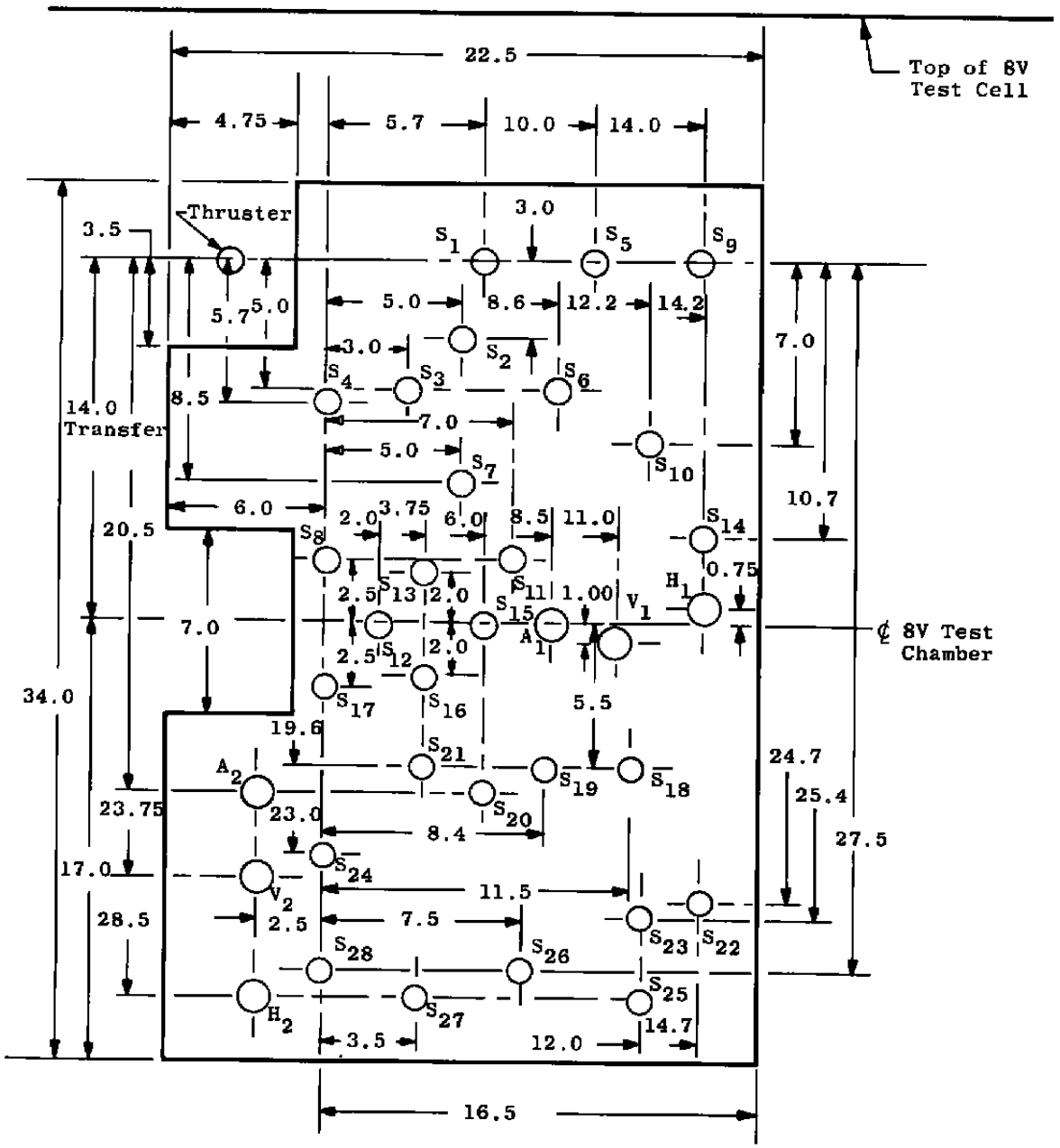

Fig. 5 Detail Dimensions of Panel 1

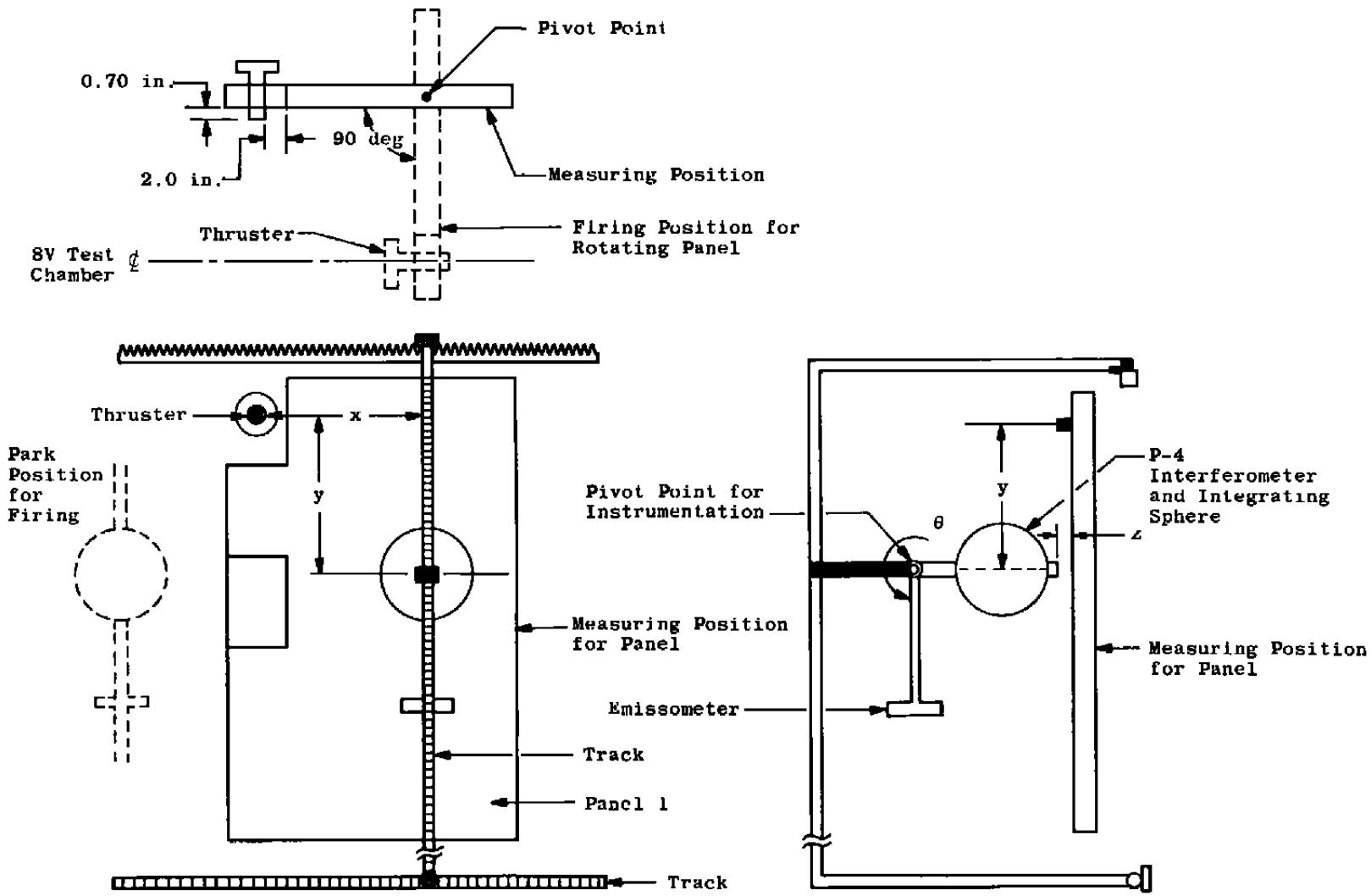

Fig. 6 Scanner Mechanism with Instrumentation

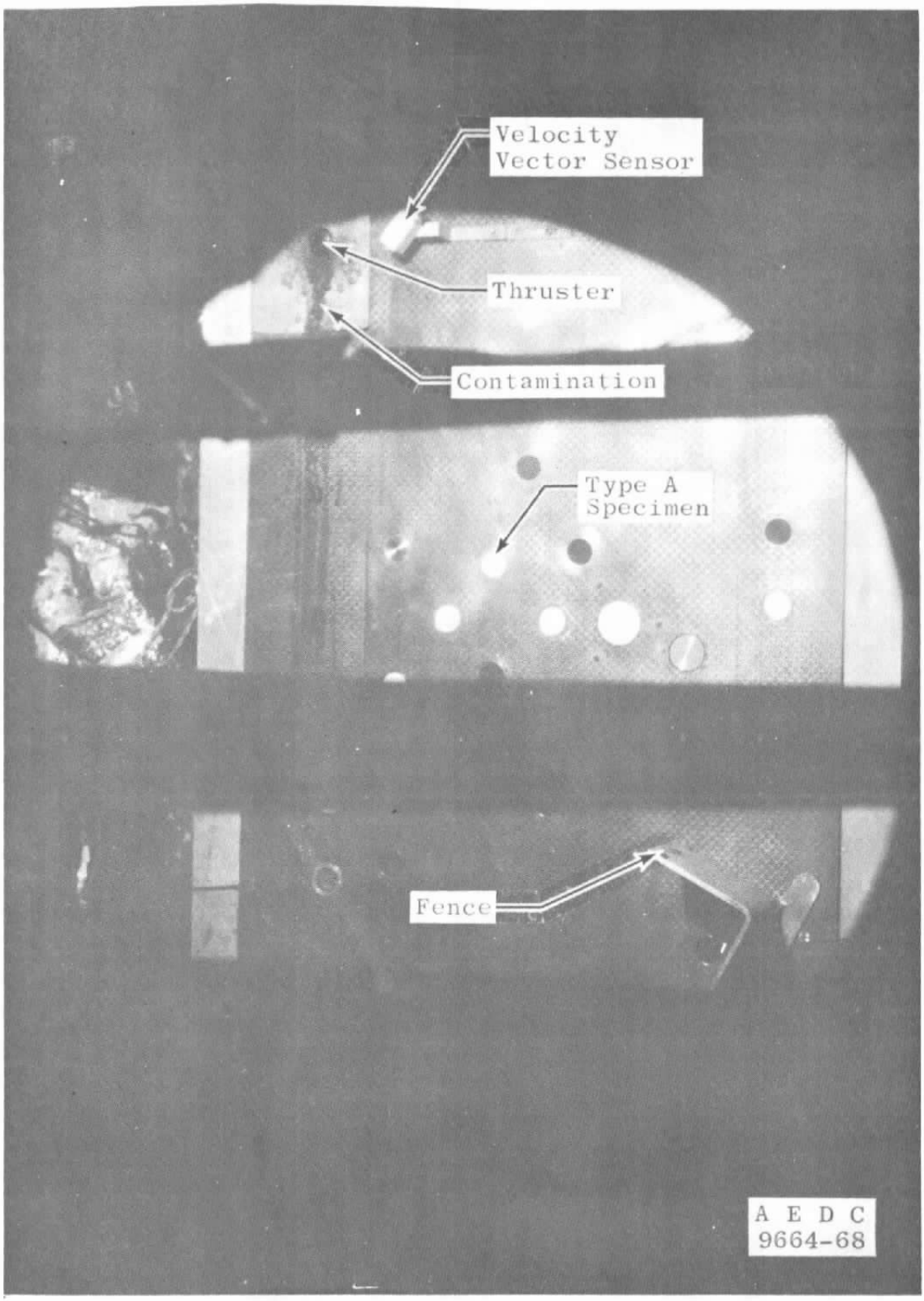

Fig. 7 Test Panel in the In Situ Measuring Position

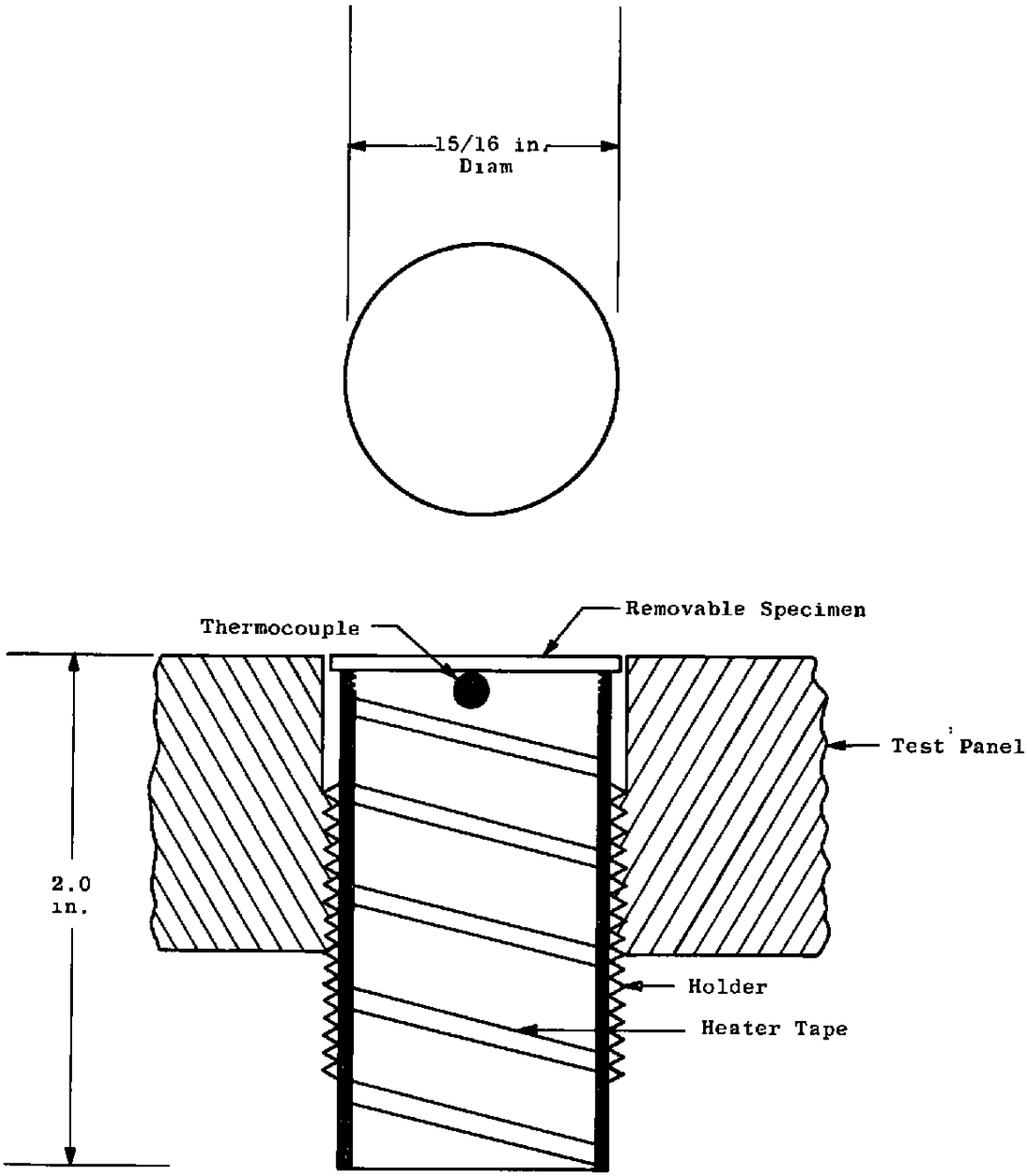

Fig. 8 Test Specimen and Holder

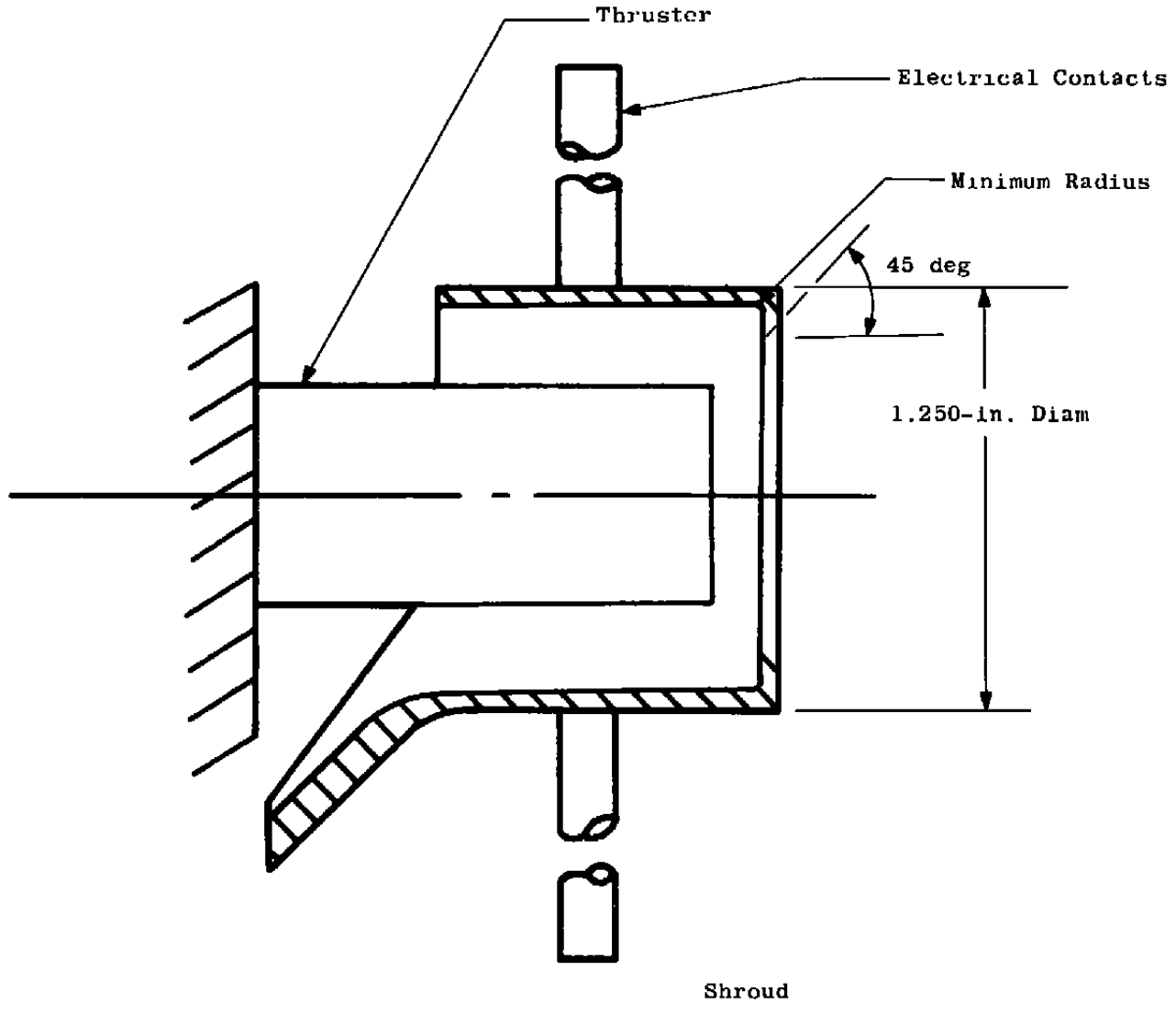

Fig. 9 Nozzle Shroud Configuration

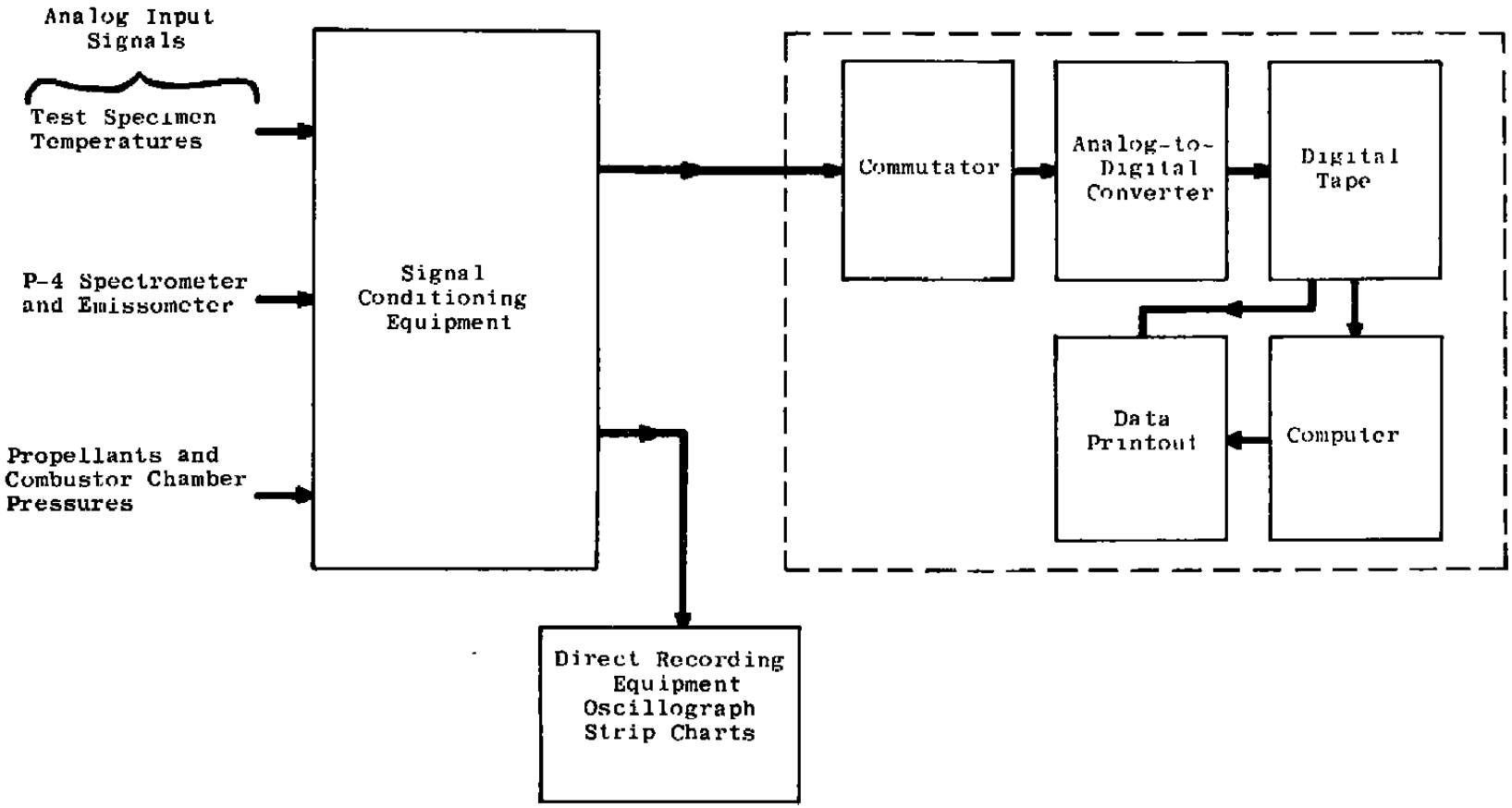

Fig. 10 Test Data System

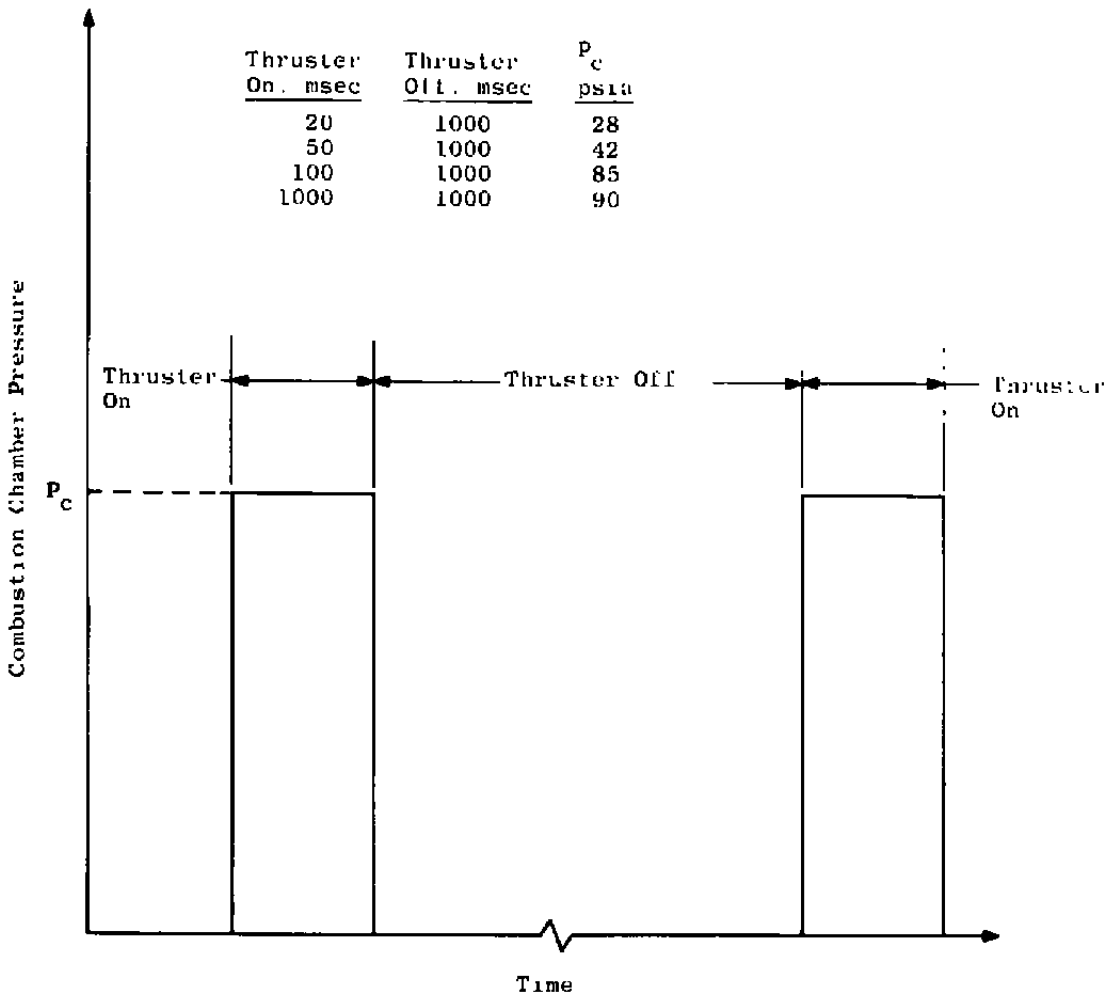

Fig. 11 Combustion Chamber Pressure versus Time

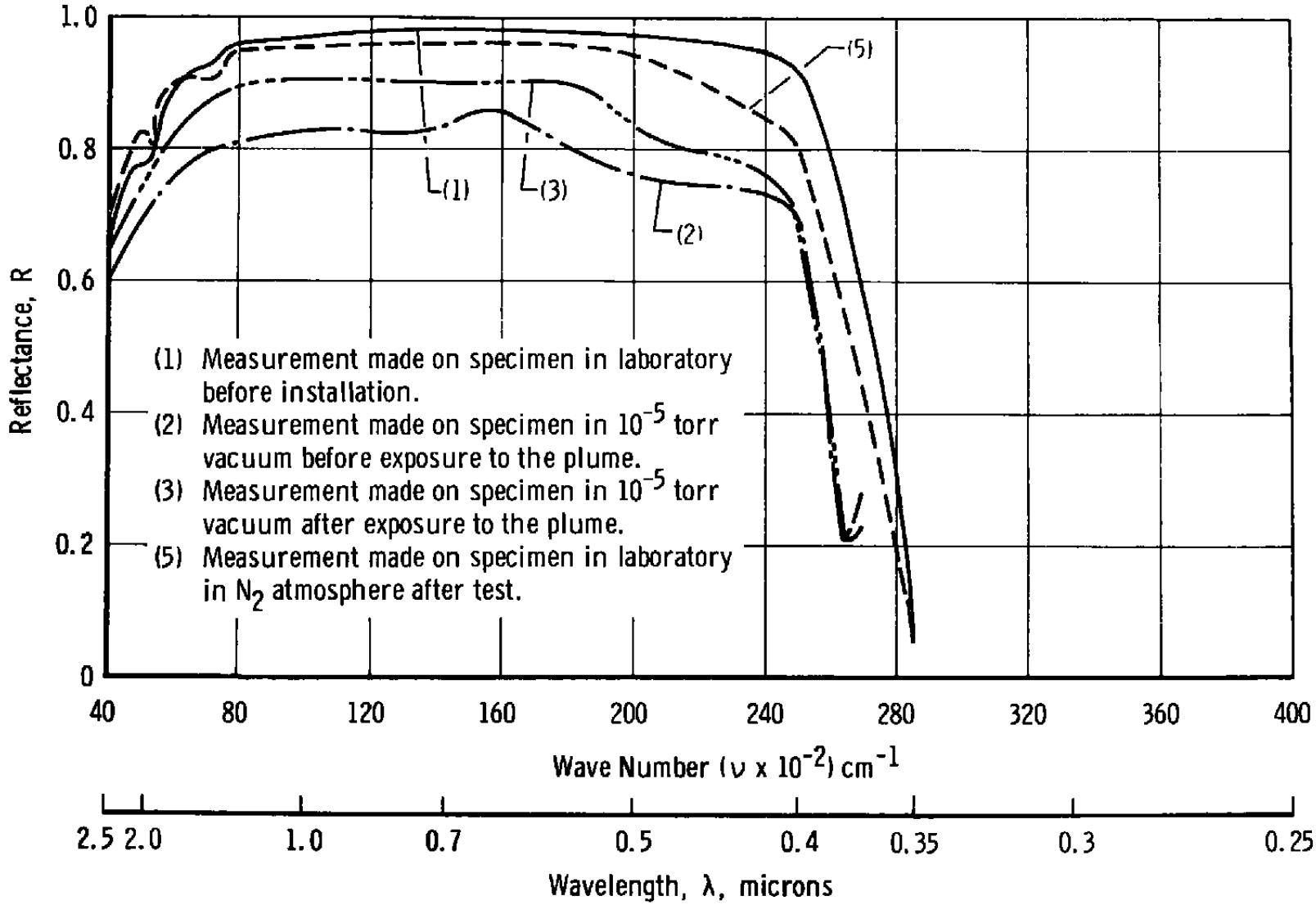

Fig. 14 Test 17—Reflectance Measurements on Specimen, Location S_2, Type A

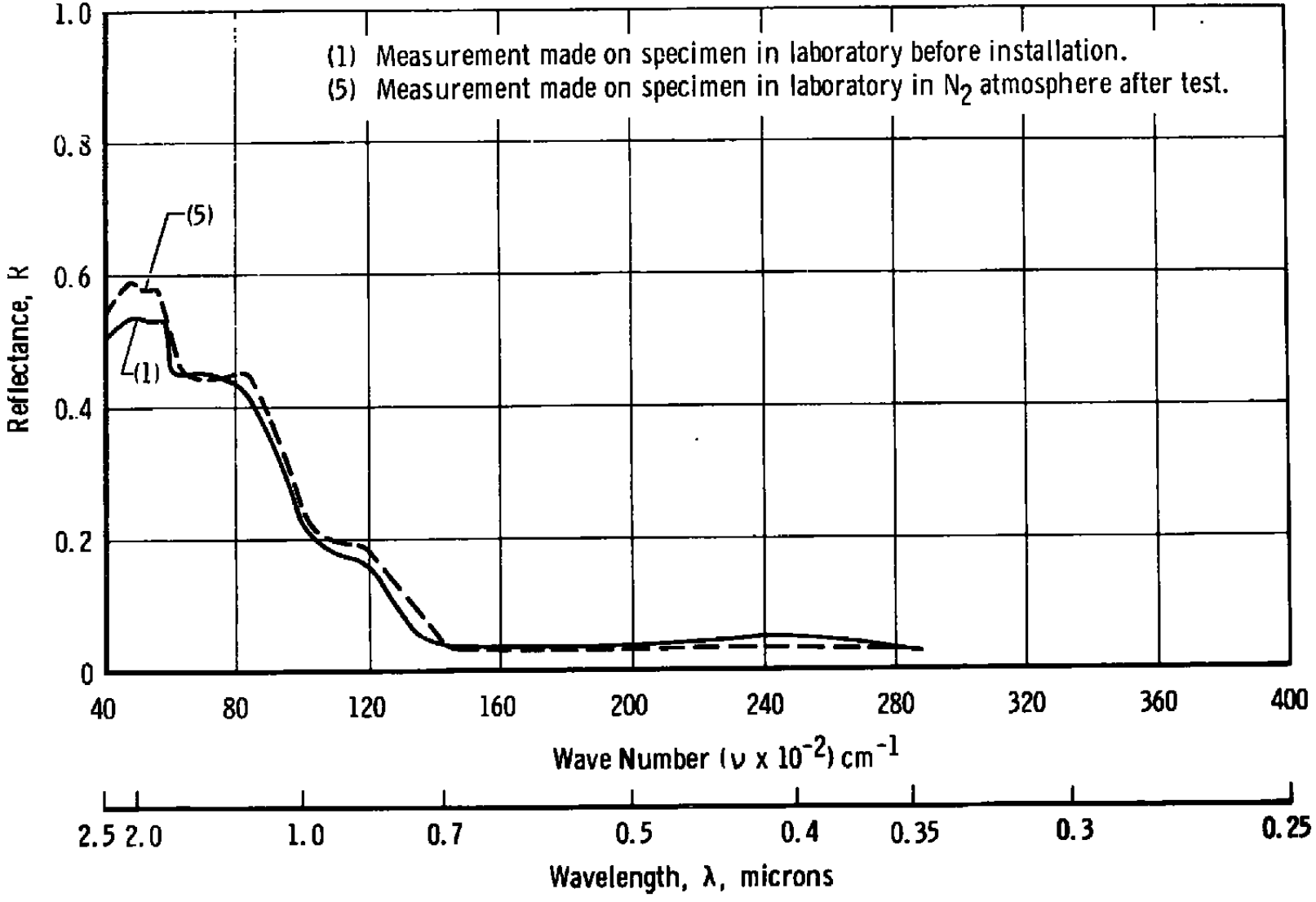

Fig. 15 Test 17—Reflectance Measurements on Specimen, Location S_7, Type K

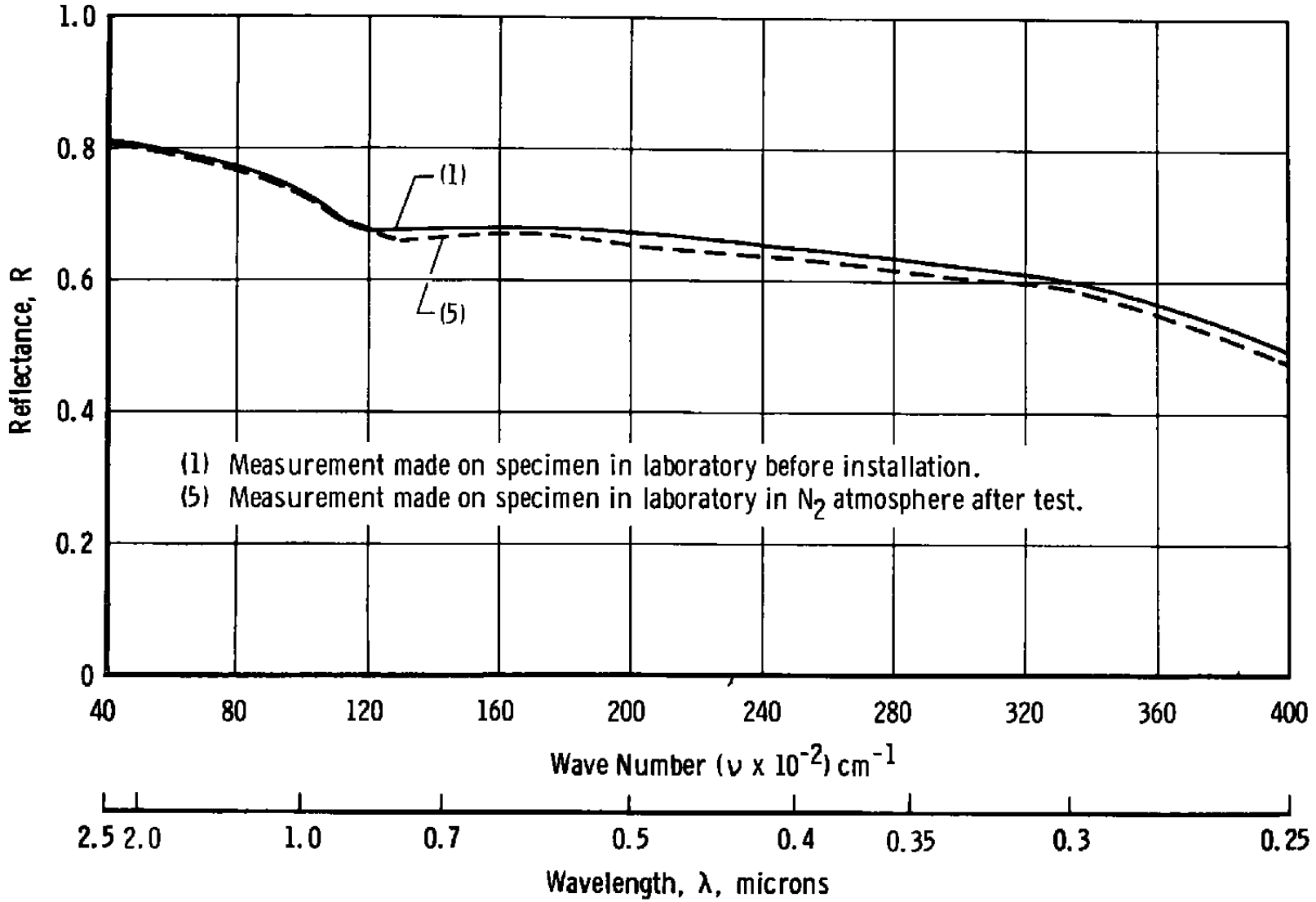

Fig. 16 Type 17--Reflectance Measurements on Specimen, Location S_8, Type D

AEDC-TR-69-175

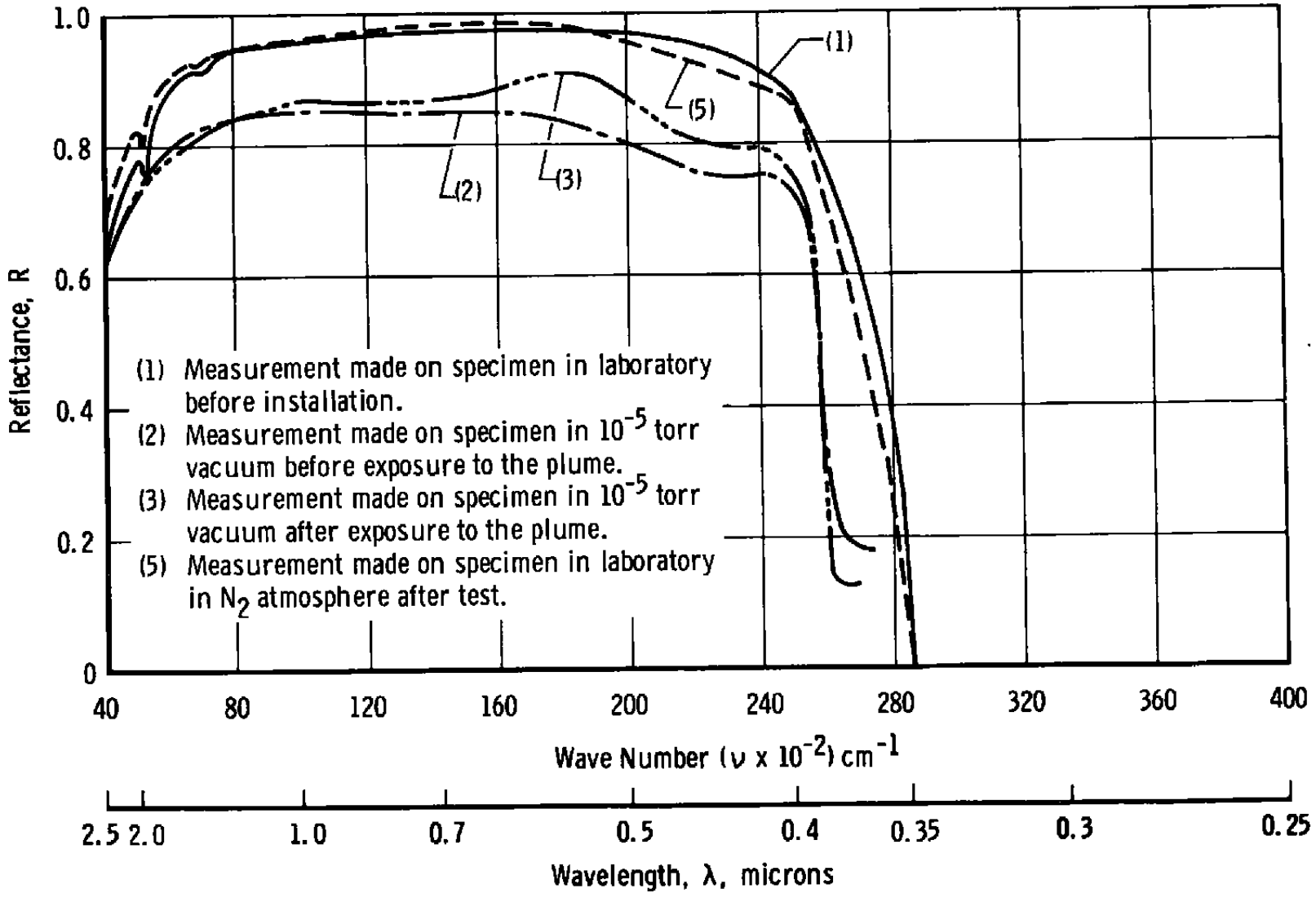

Fig. 17 Test 17—Reflectance Measurements on Specimen, Location S_{10}, Type A

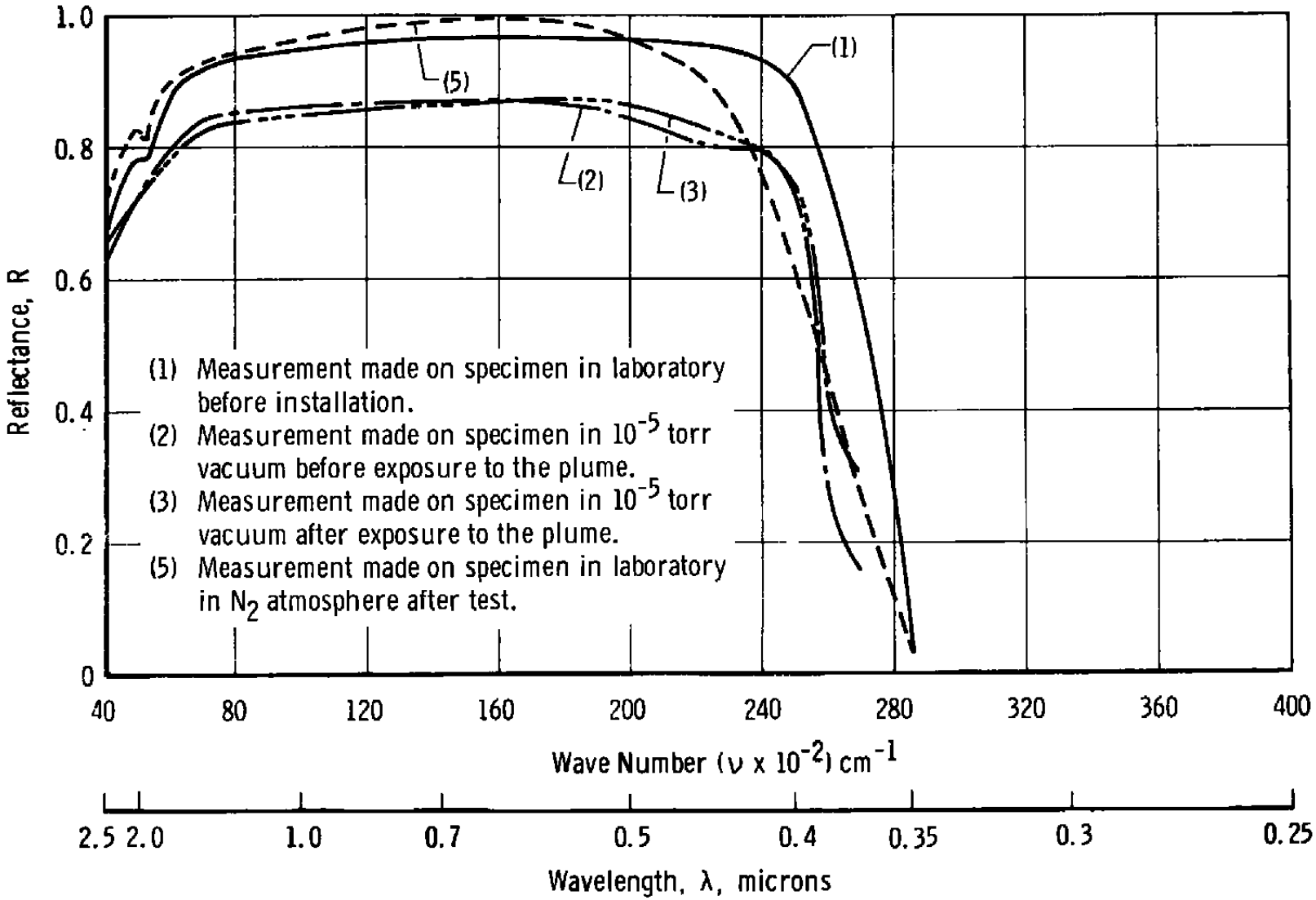

Fig. 18 Test 17—Reflectance Measurements on Specimen, Location S_{17}, Type A

AEDC-TR-69-175

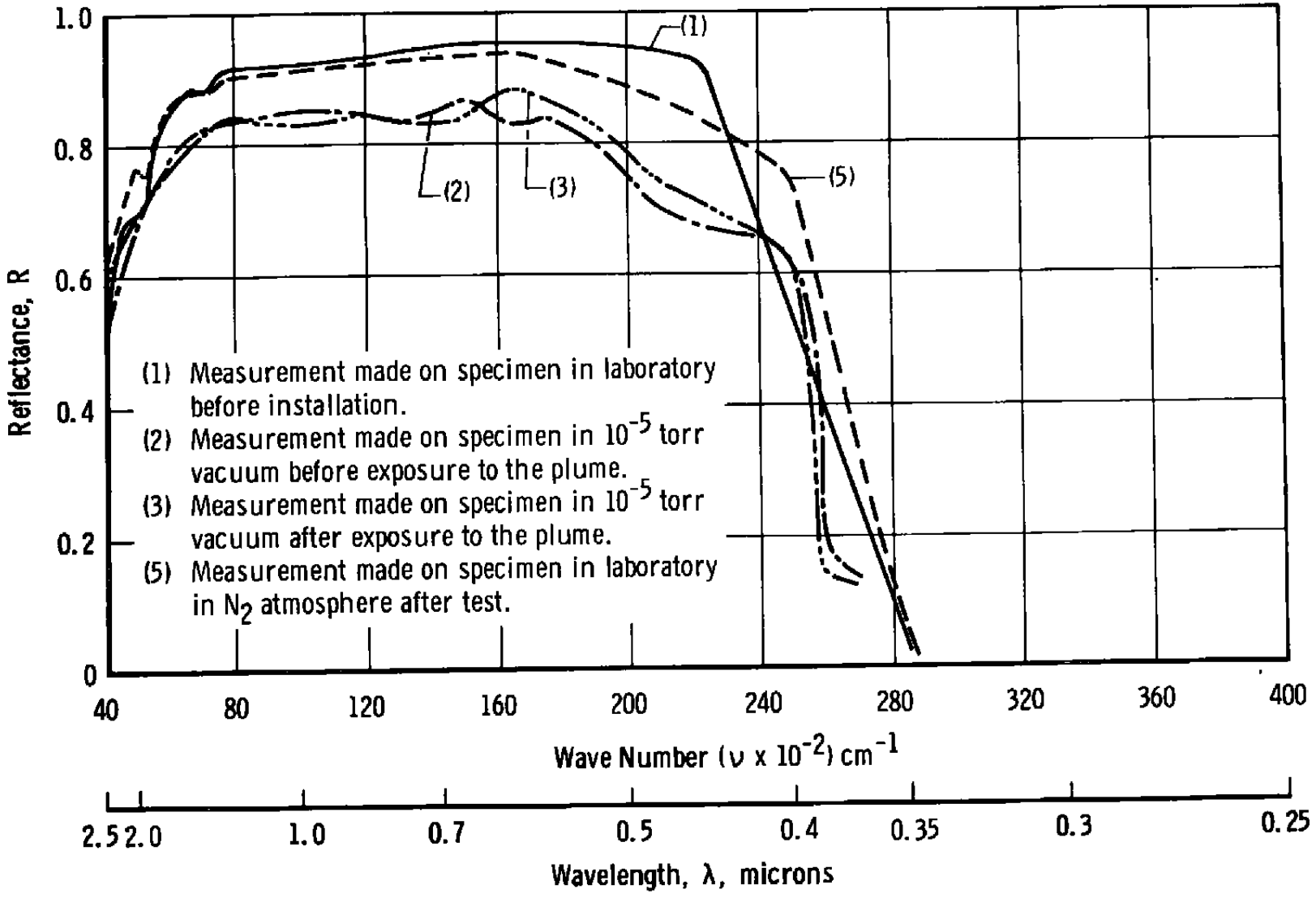

Fig. 19 Test 17—Reflectance Measurements on Specimen, Location S_{19}, Type A

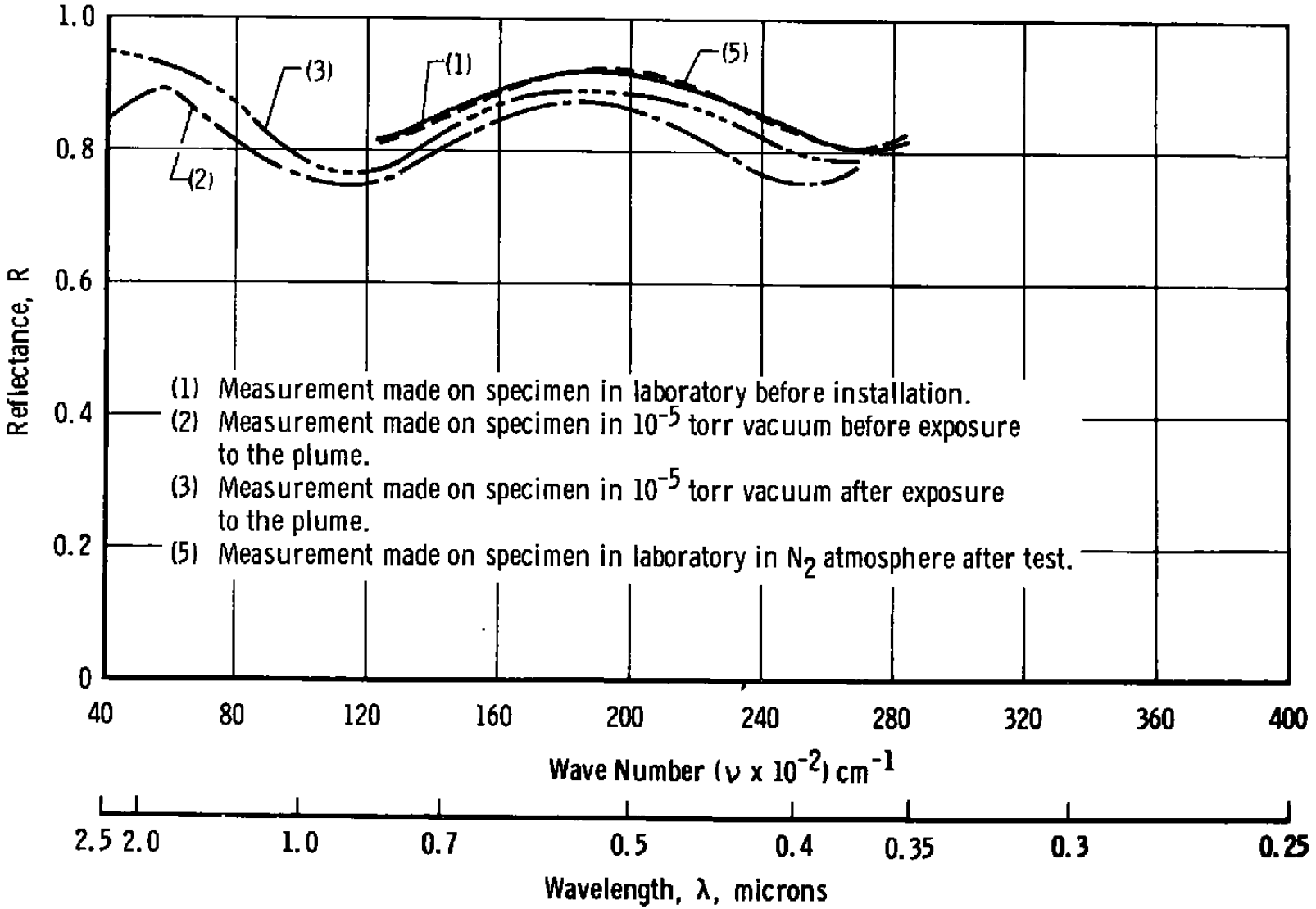

Fig. 20 Test 17—Reflectance Measurements on Specimen, Location S_{24}, Mirror

AEDC-TR-69-175

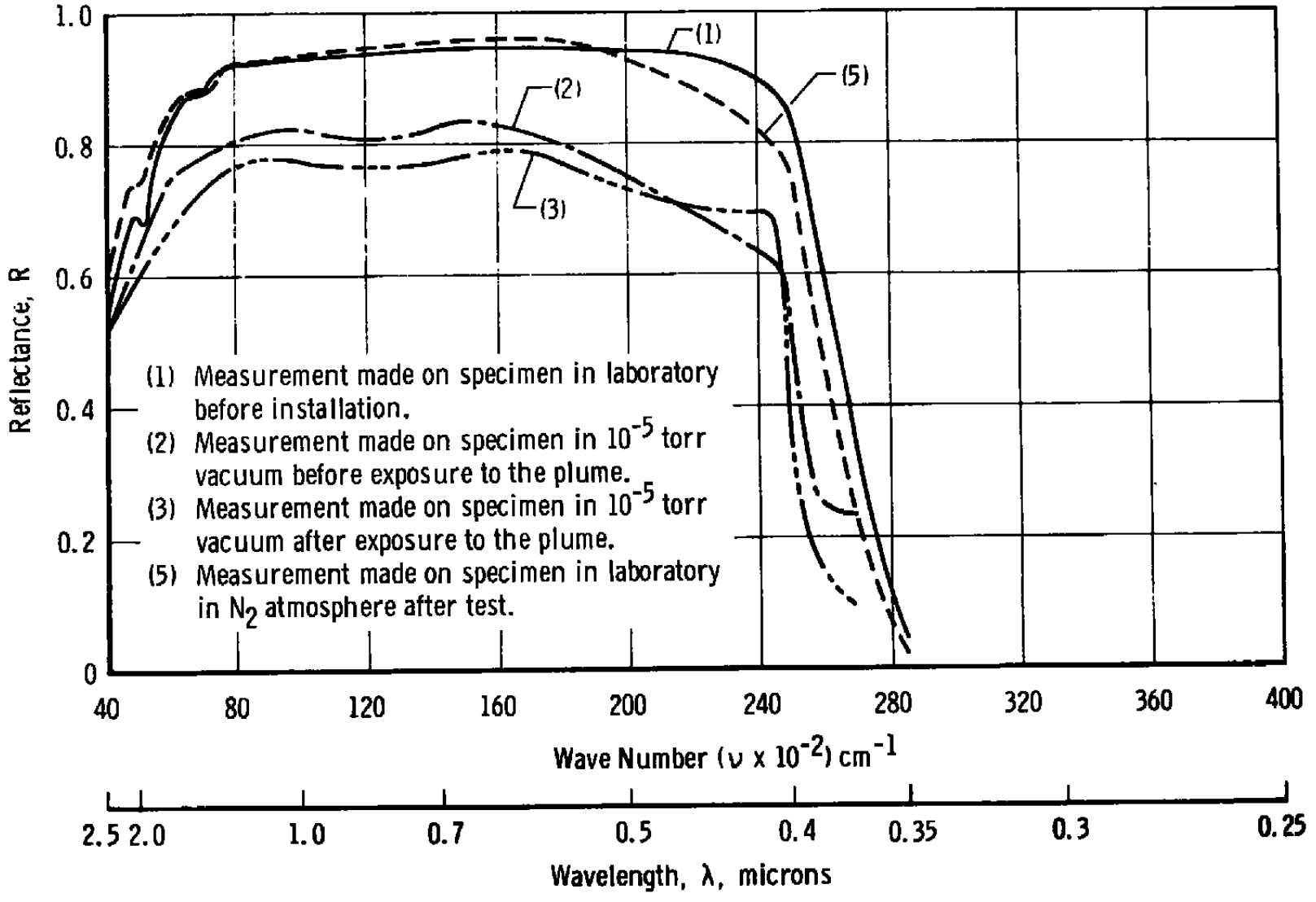

Fig. 21 Test 17—Reflectance Measurements on Specimen, Location S_{28}, Type A

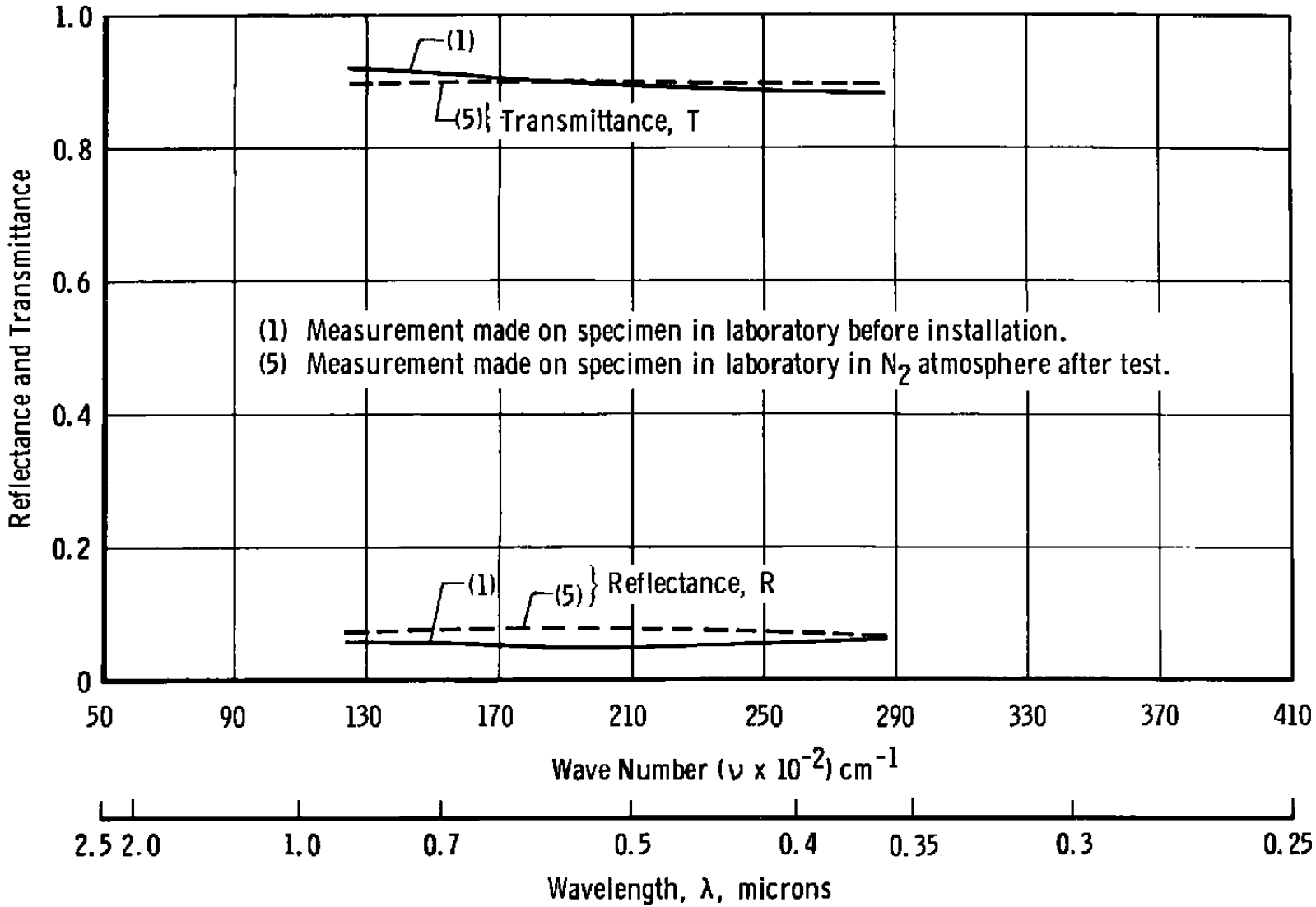

Fig. 22 Test 17—Reflectance and Transmittance Measurements on Specimen, Location S_{27}, Window

AEDC-TR-69-175

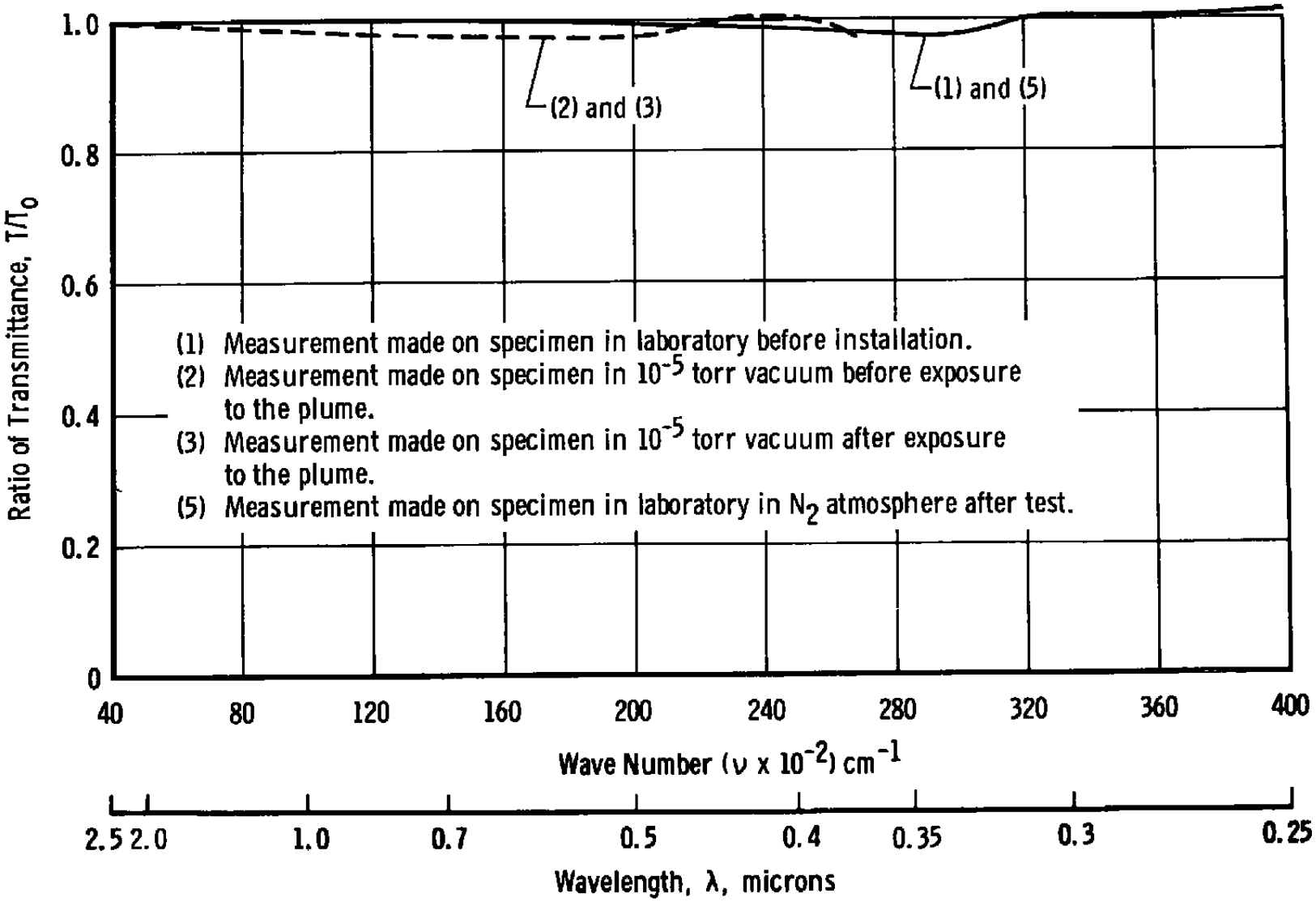

Fig. 23 Test 17—Transmittance Measurements on Specimen, Location V_2, View Port Window

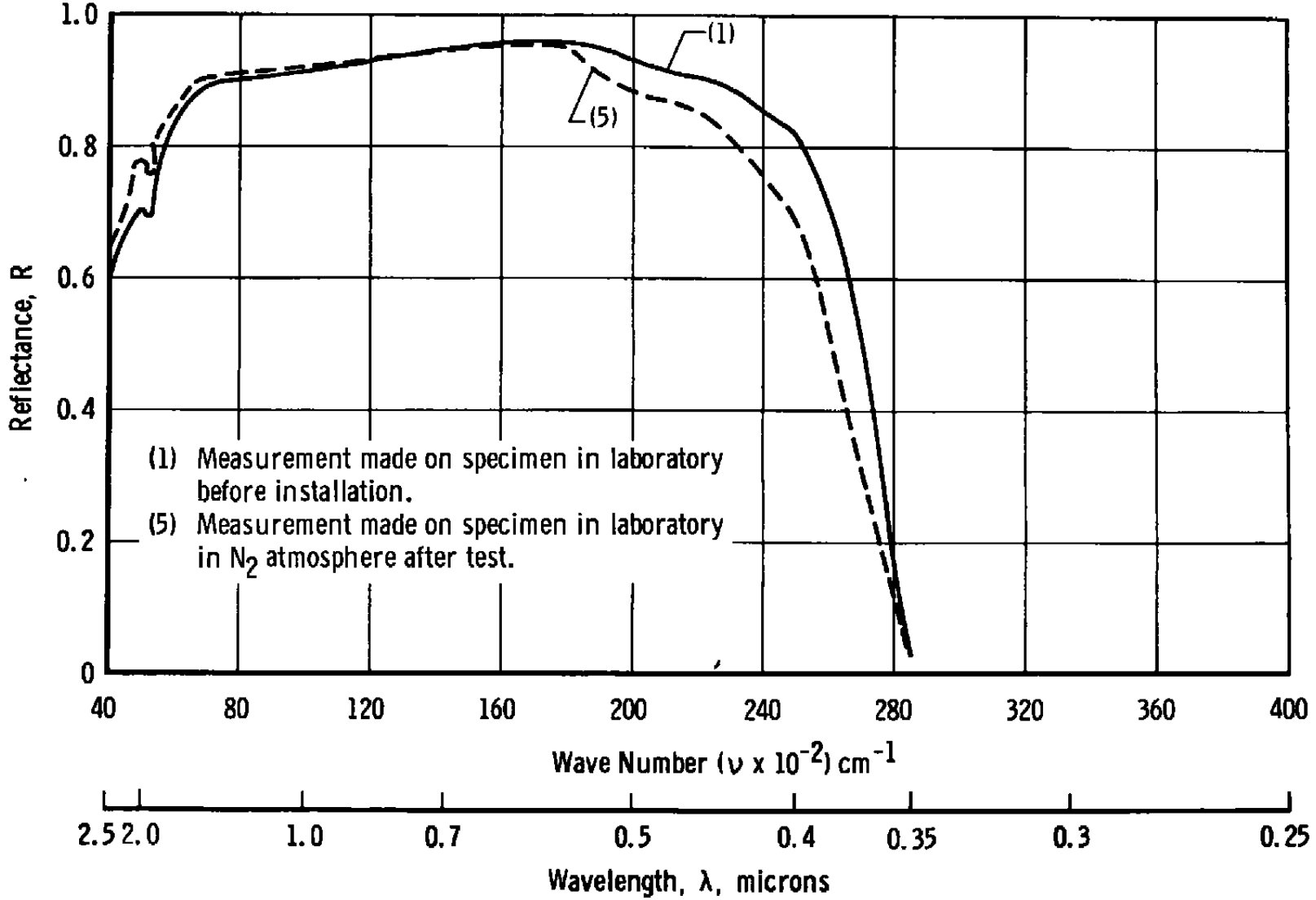

Fig. 24 Test 18—Reflectance Measurements on Specimen, Location S_2, Type A

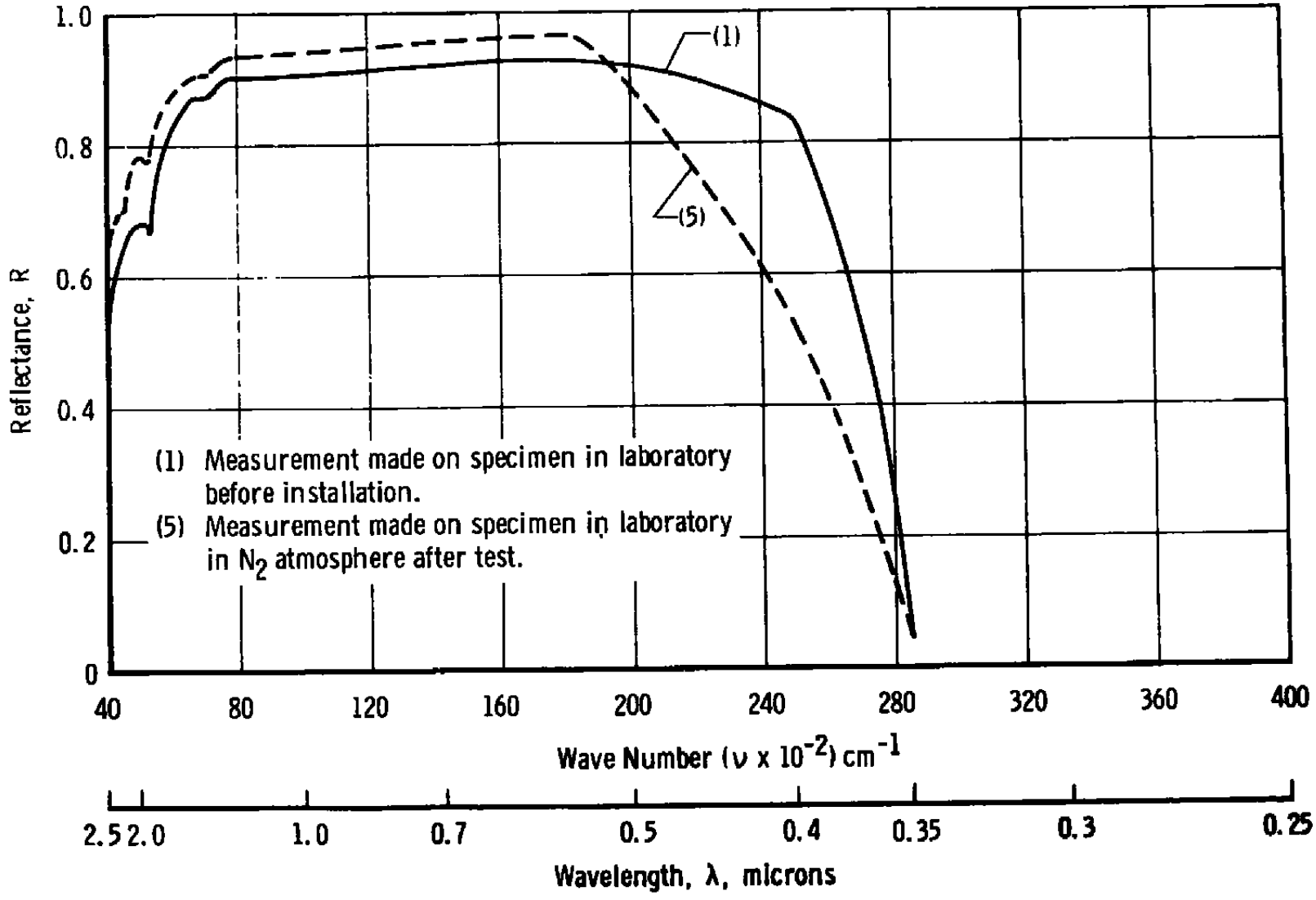

Fig. 25 Test 18—Reflectance Measurements on Specimen, Location S_3, Type A

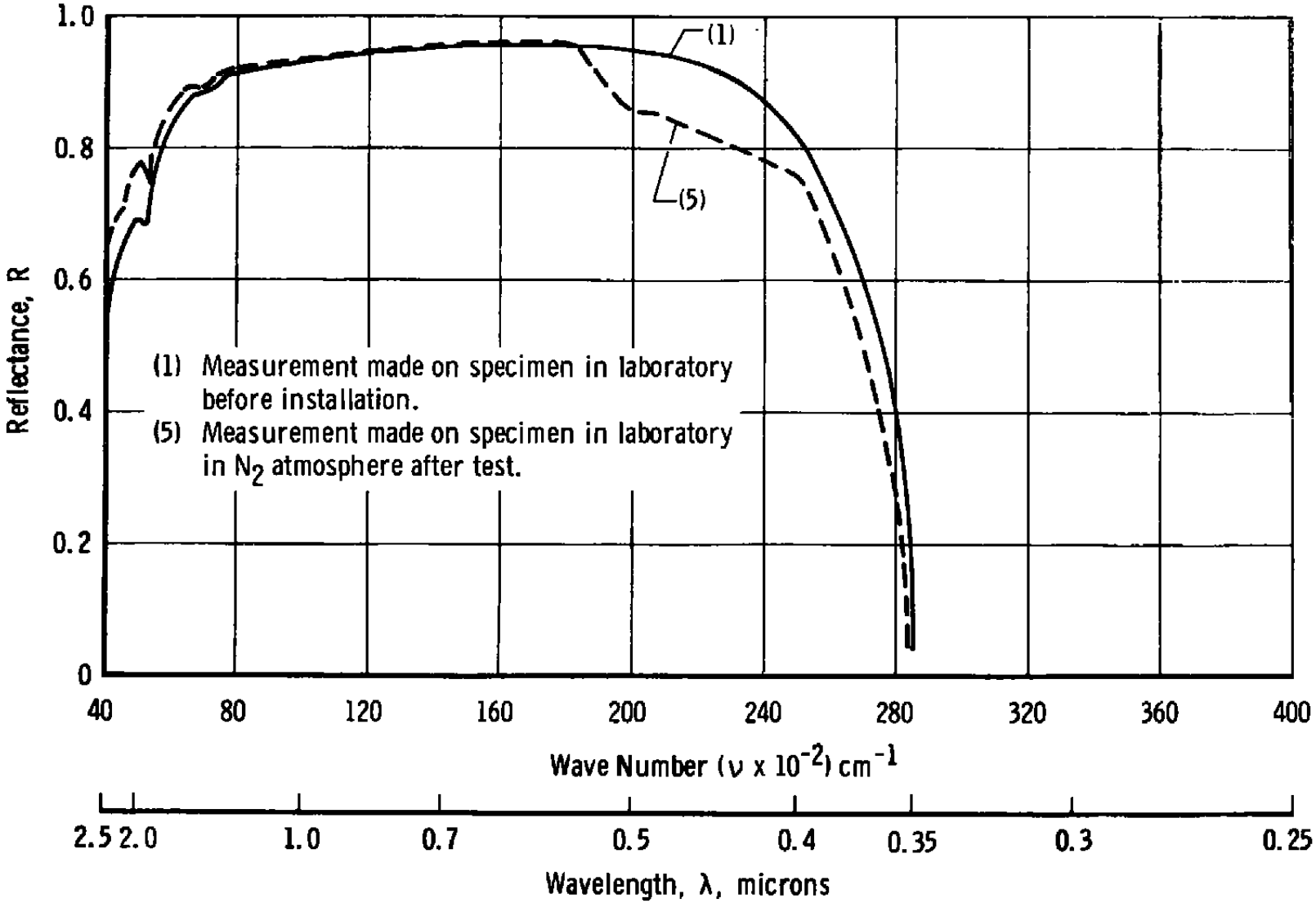

Fig. 26 Test 18--Reflectance Measurements on Specimen, Location S_3, Type A

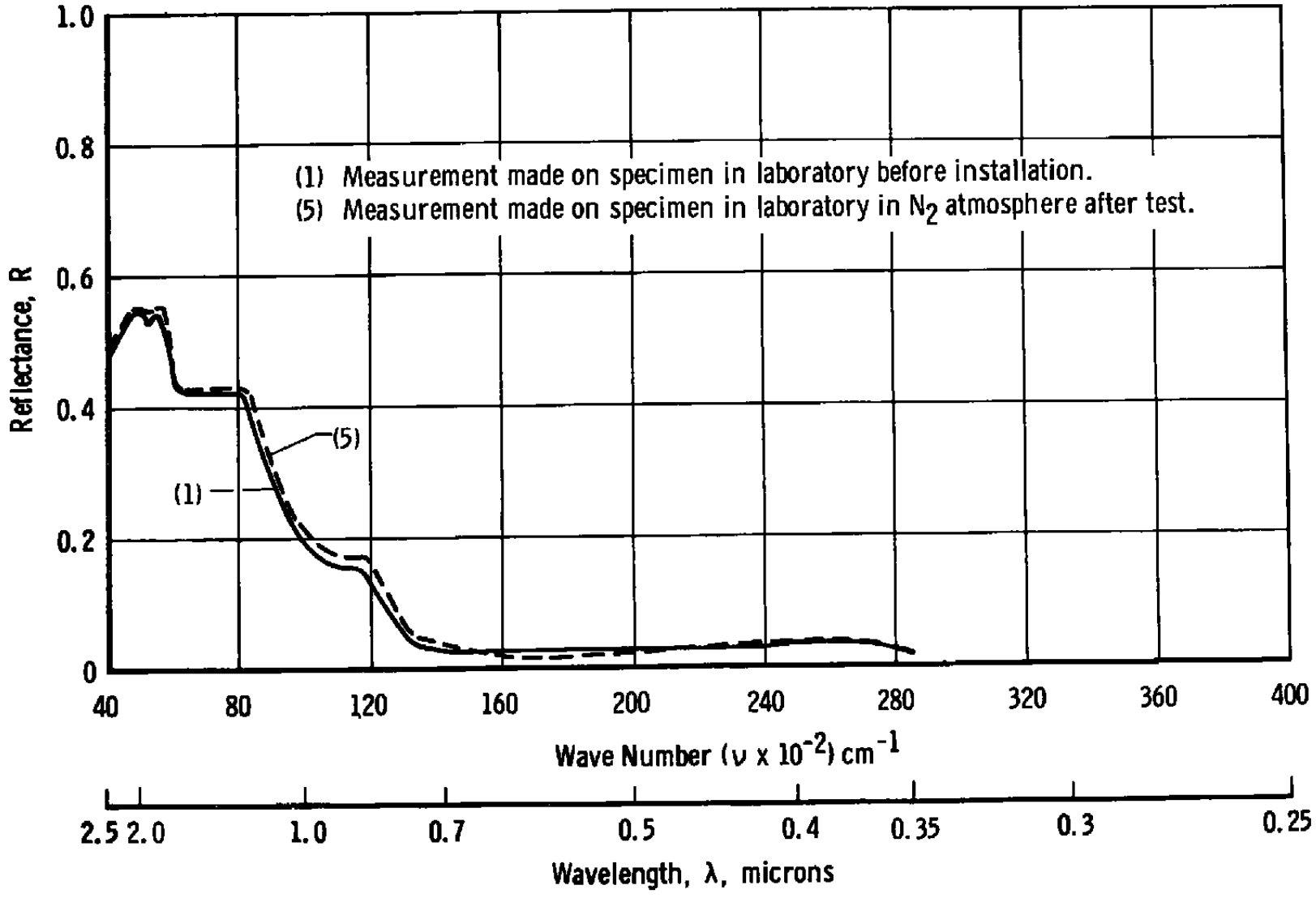

Fig. 27 Test 18—Reflectance Measurements on Specimen, Location S_7, Type K

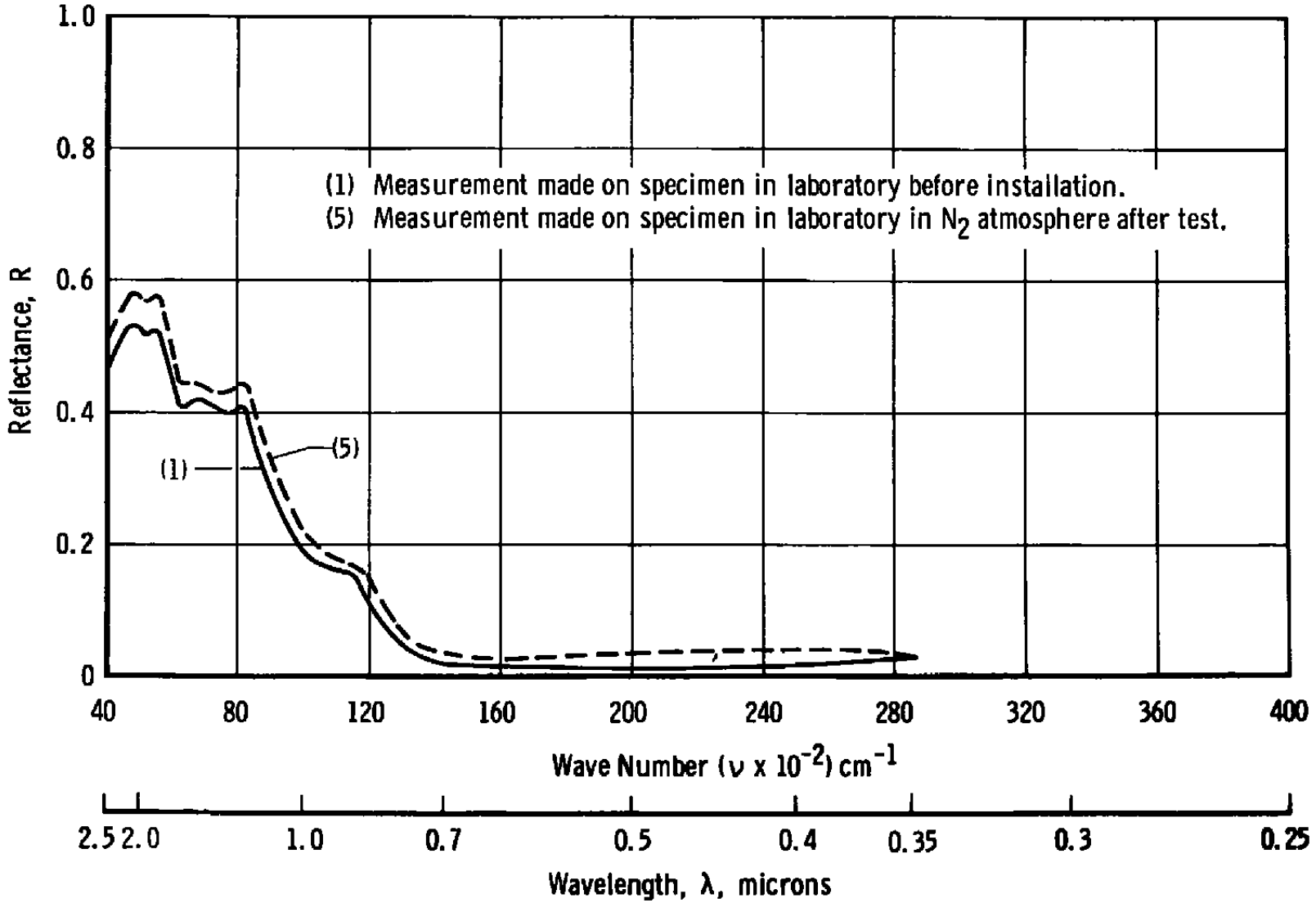

Fig. 28 Test 18—Reflectance Measurements on Specimen, Location S_{11}, Type K

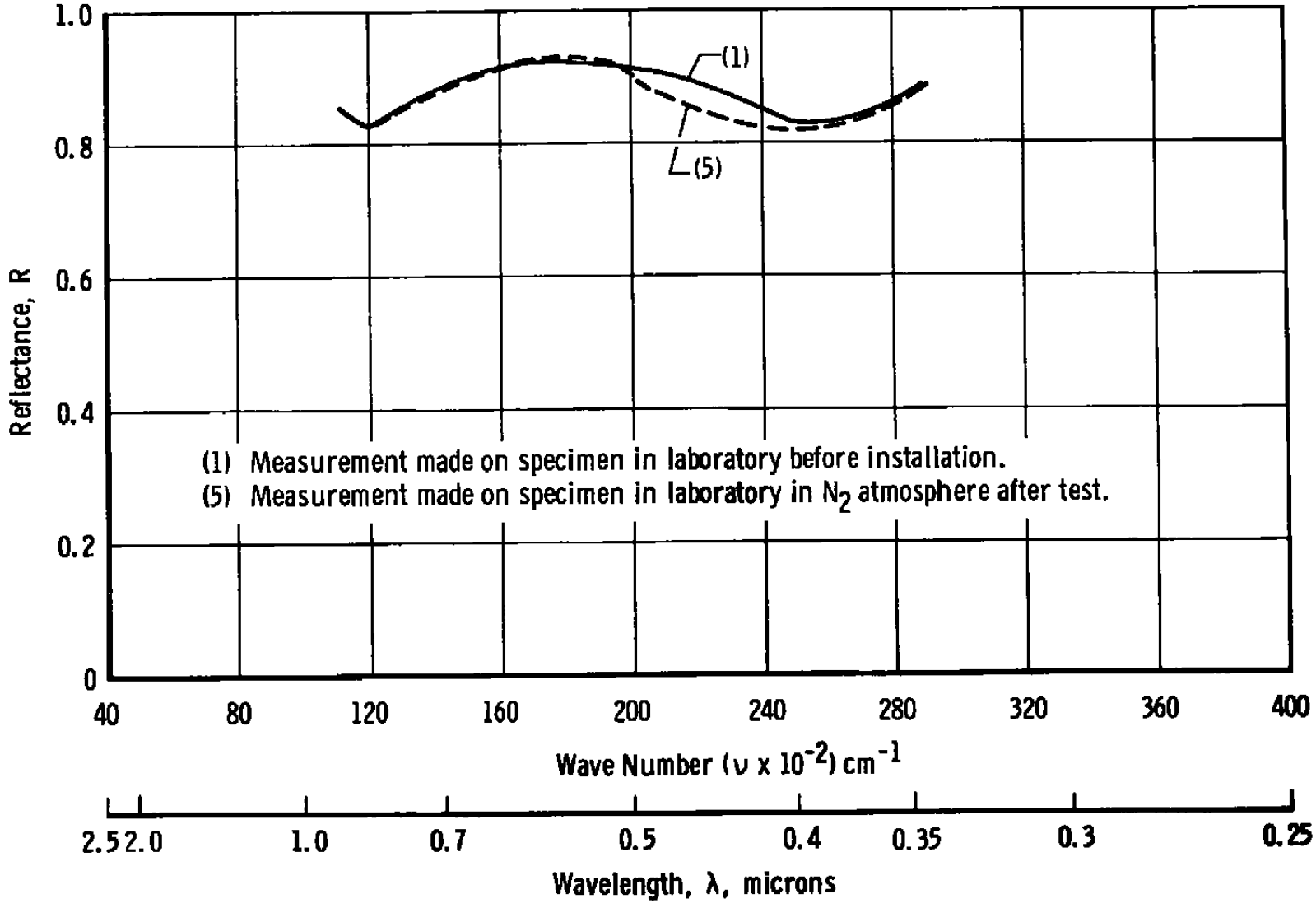

Fig. 29 Test 18—Reflectance Measurements on Specimen, Location S_{24}, Mirror

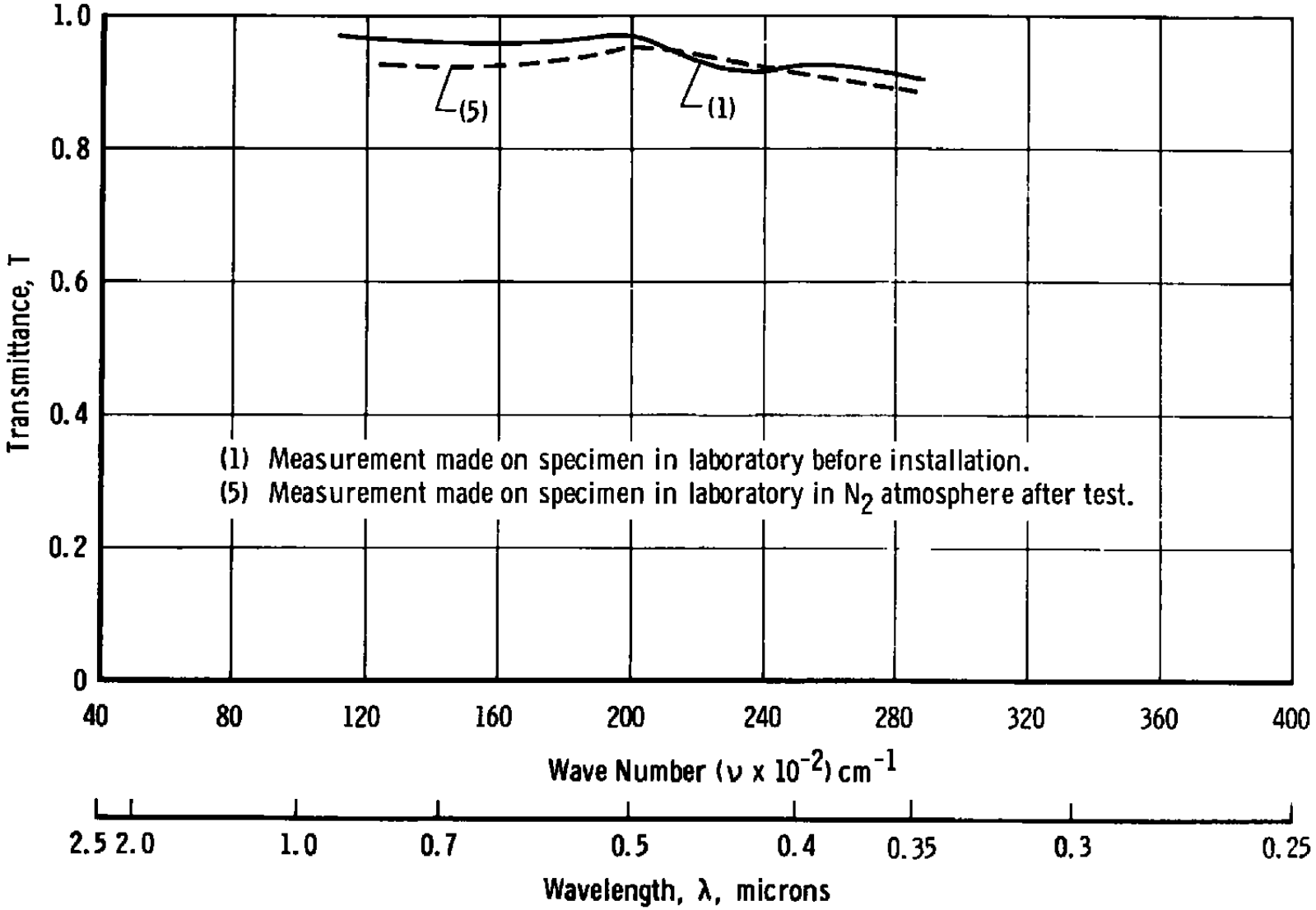

Fig. 30 Test 18—Transmittance Measurements on Specimen, Location S_{27}, Window

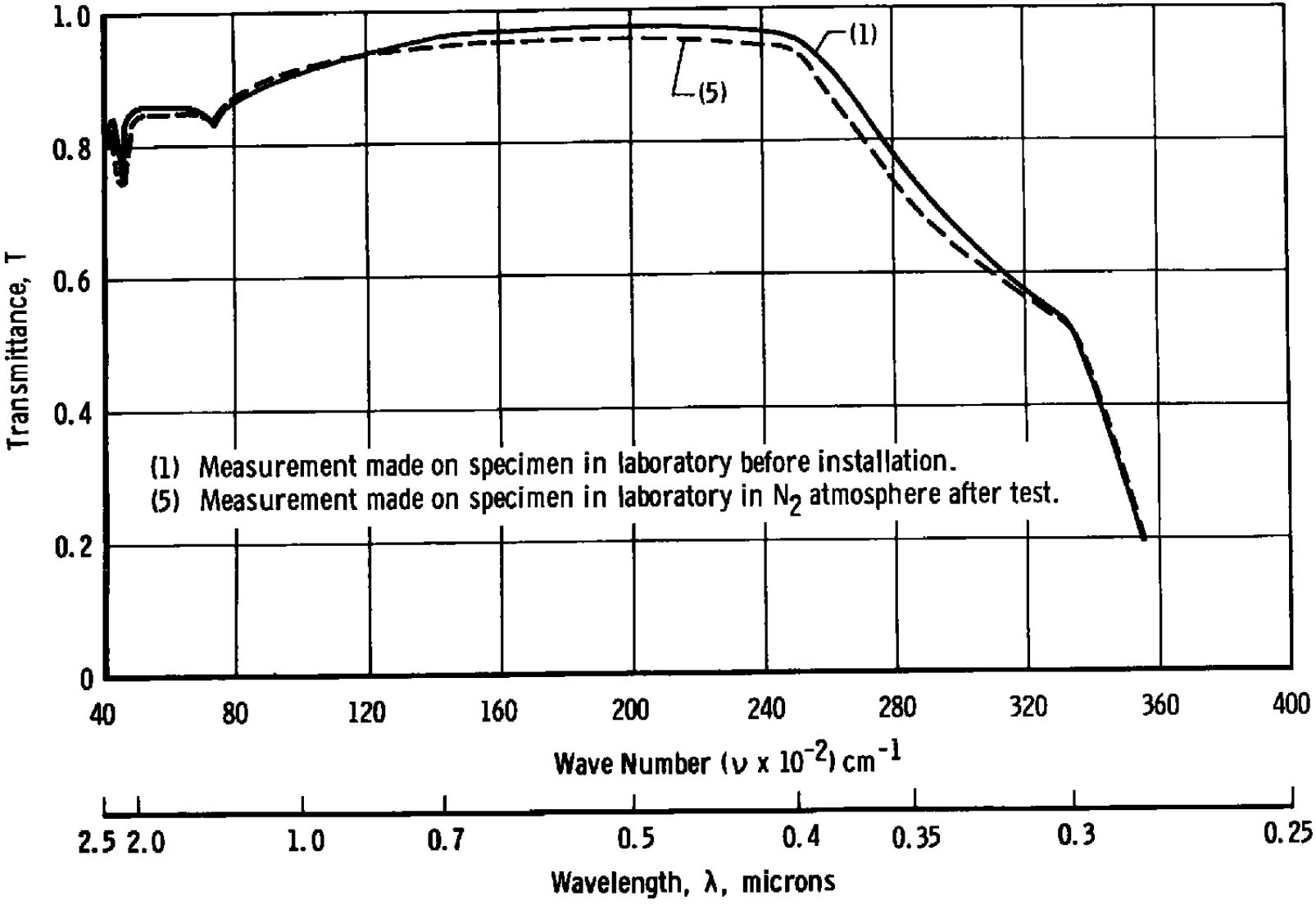

Fig. 31 Test 18—Transmittance Measurements on Specimen, Location V_2, View Port Window

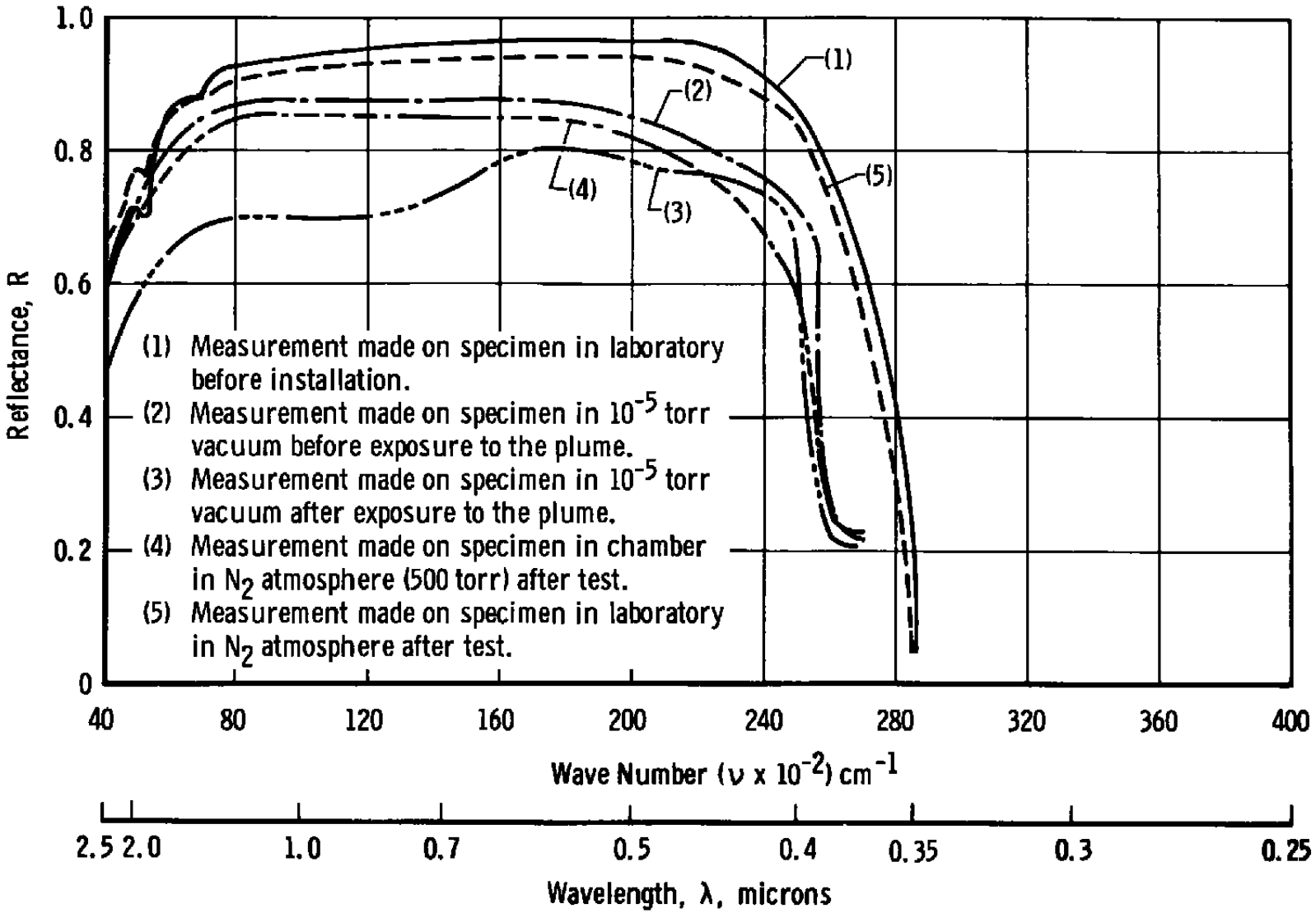

Fig. 32 Test 19—Reflectance Measurements on Specimen, Location S_2, Type A

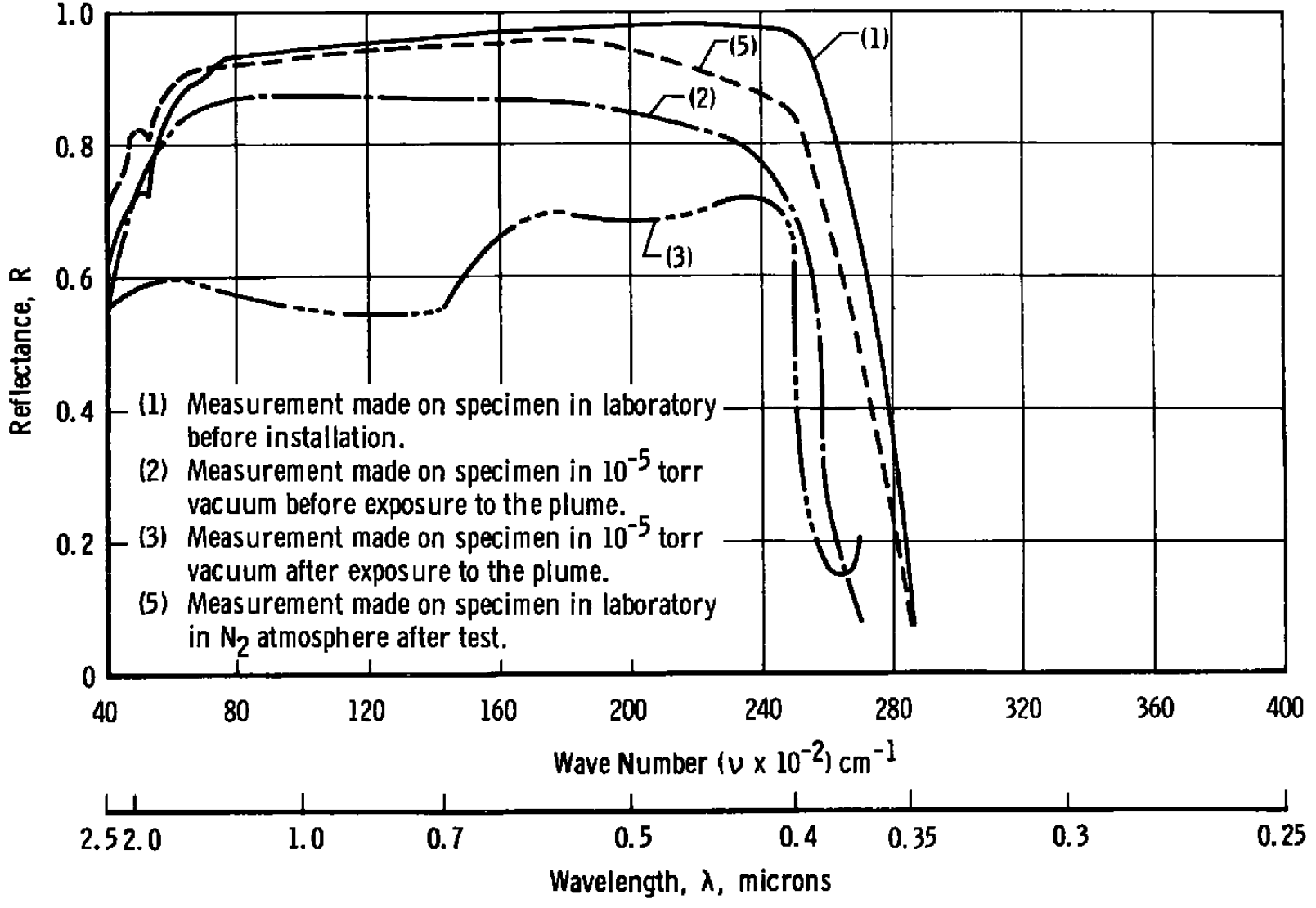

Fig. 33 Test 19—Reflectance Measurements on Specimen, Location S_4, Type A

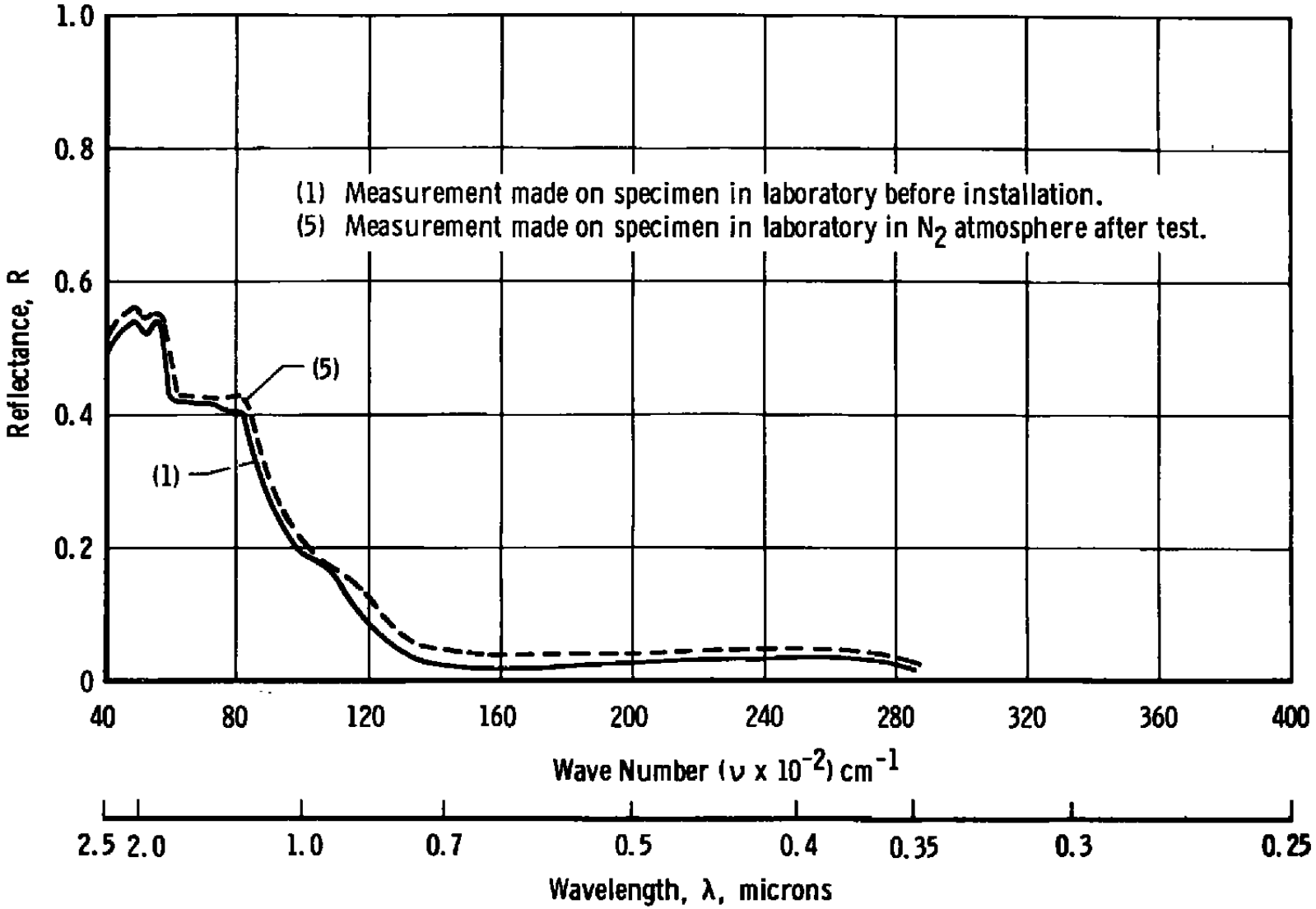

Fig. 34 Test 19—Reflectance Measurements on Specimen, Location S_7, Type K

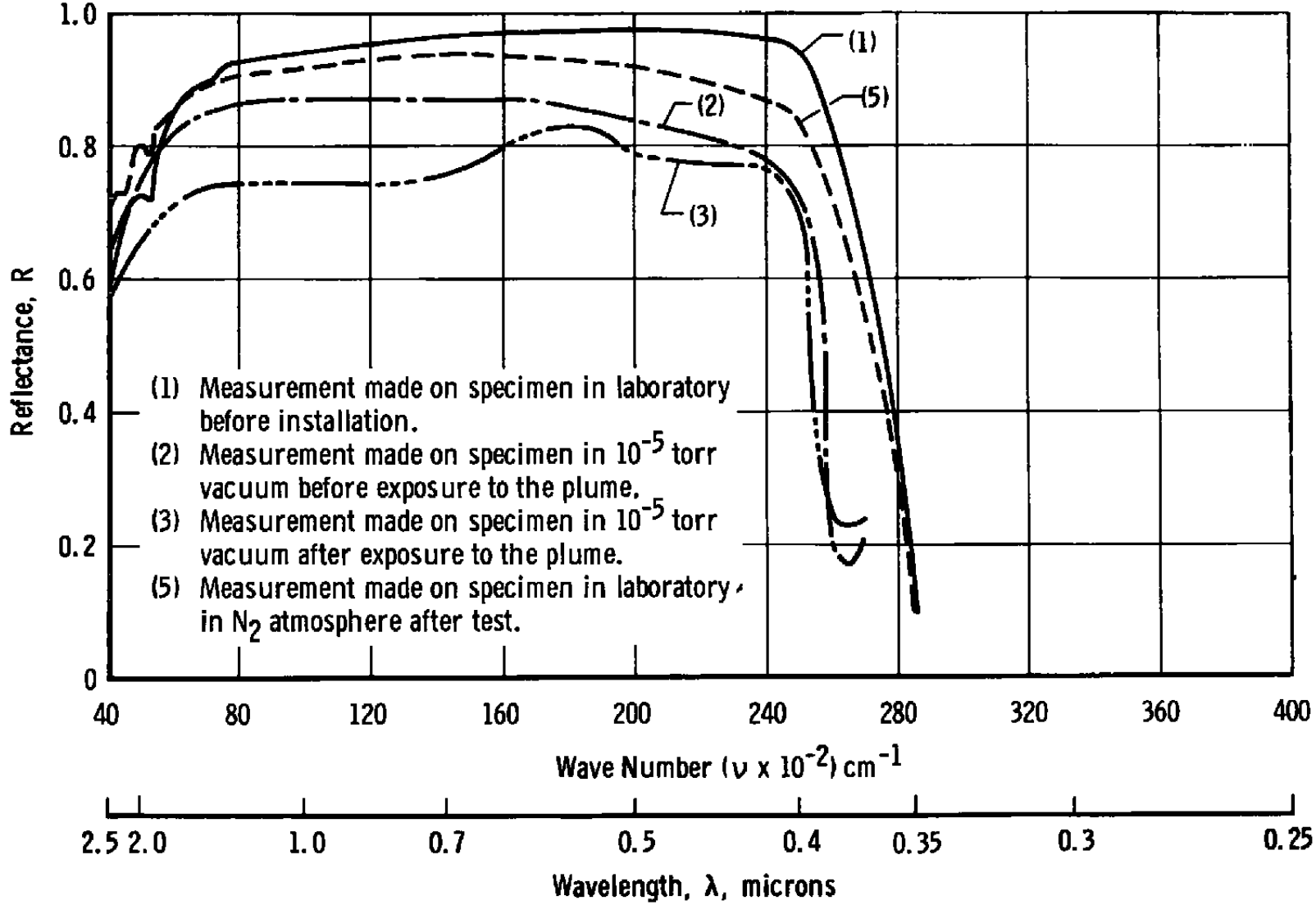

Fig. 35 Test 19—Reflectance Measurements on Specimen, Location S_{10}, Type A

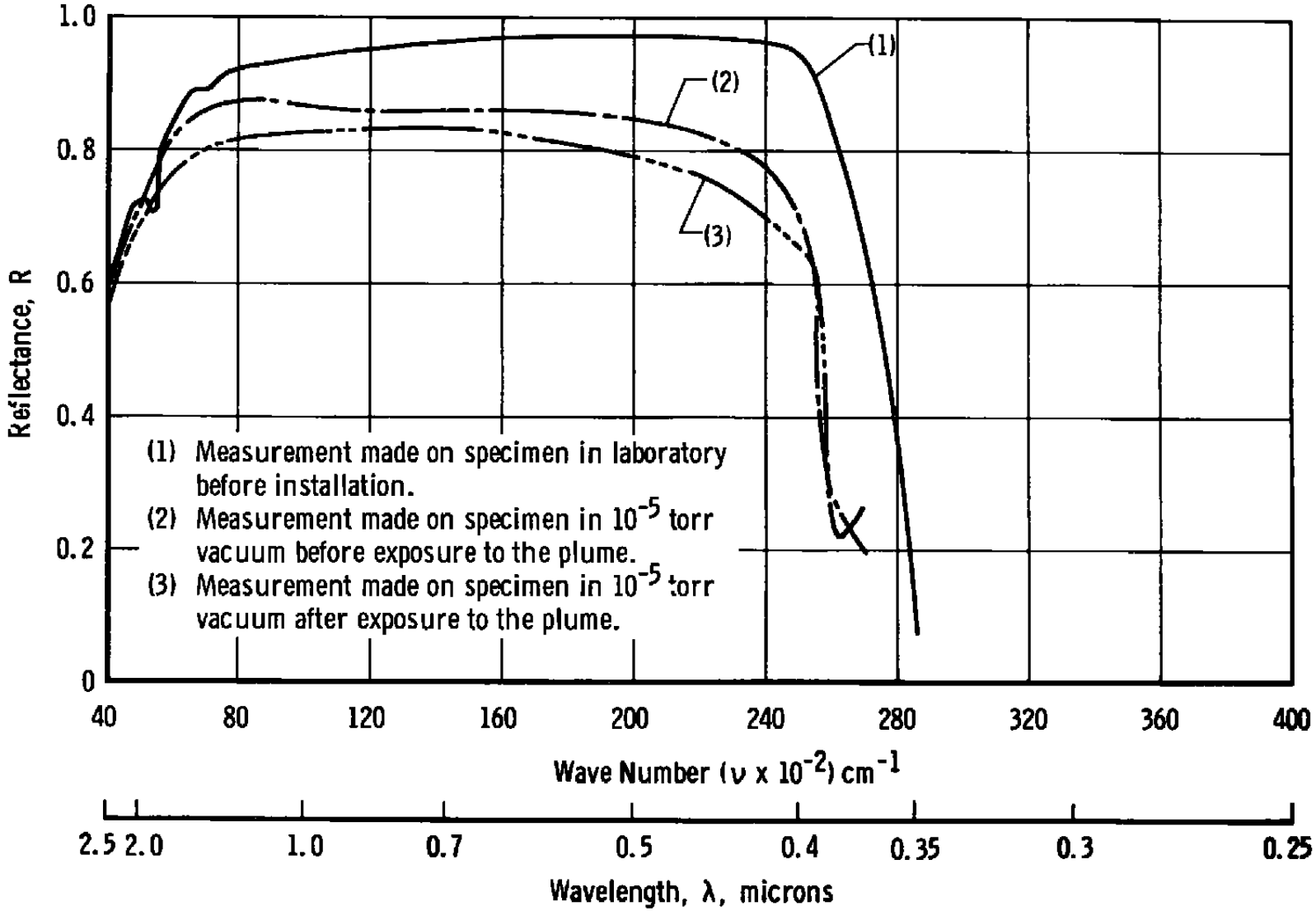

Fig. 36 Test 19—Reflectance Measurements on Specimen, Location S_{15}, Type A

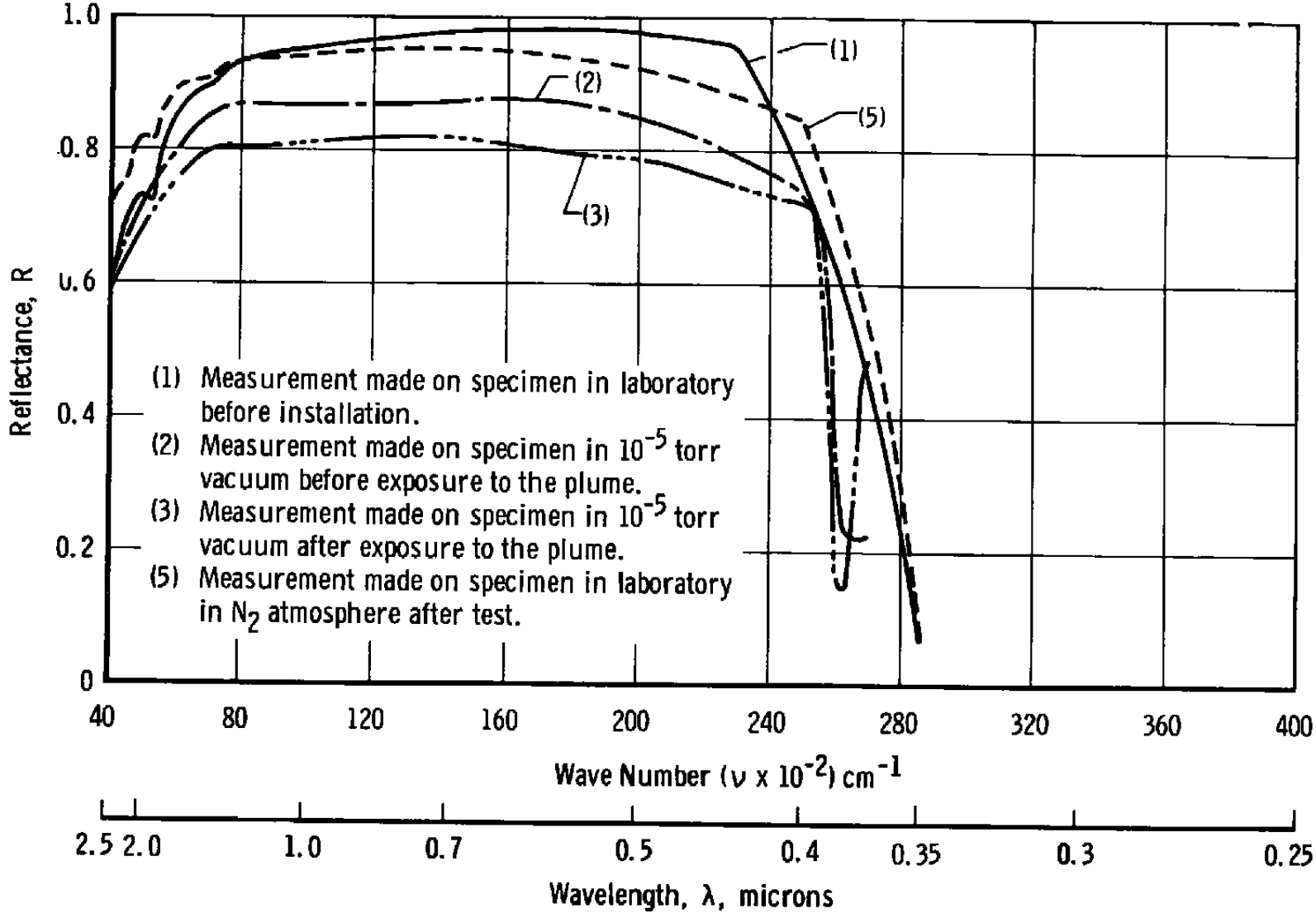

Fig. 37 Test 19—Reflectance Measurements on Specimen, Location S_{17}, Type A

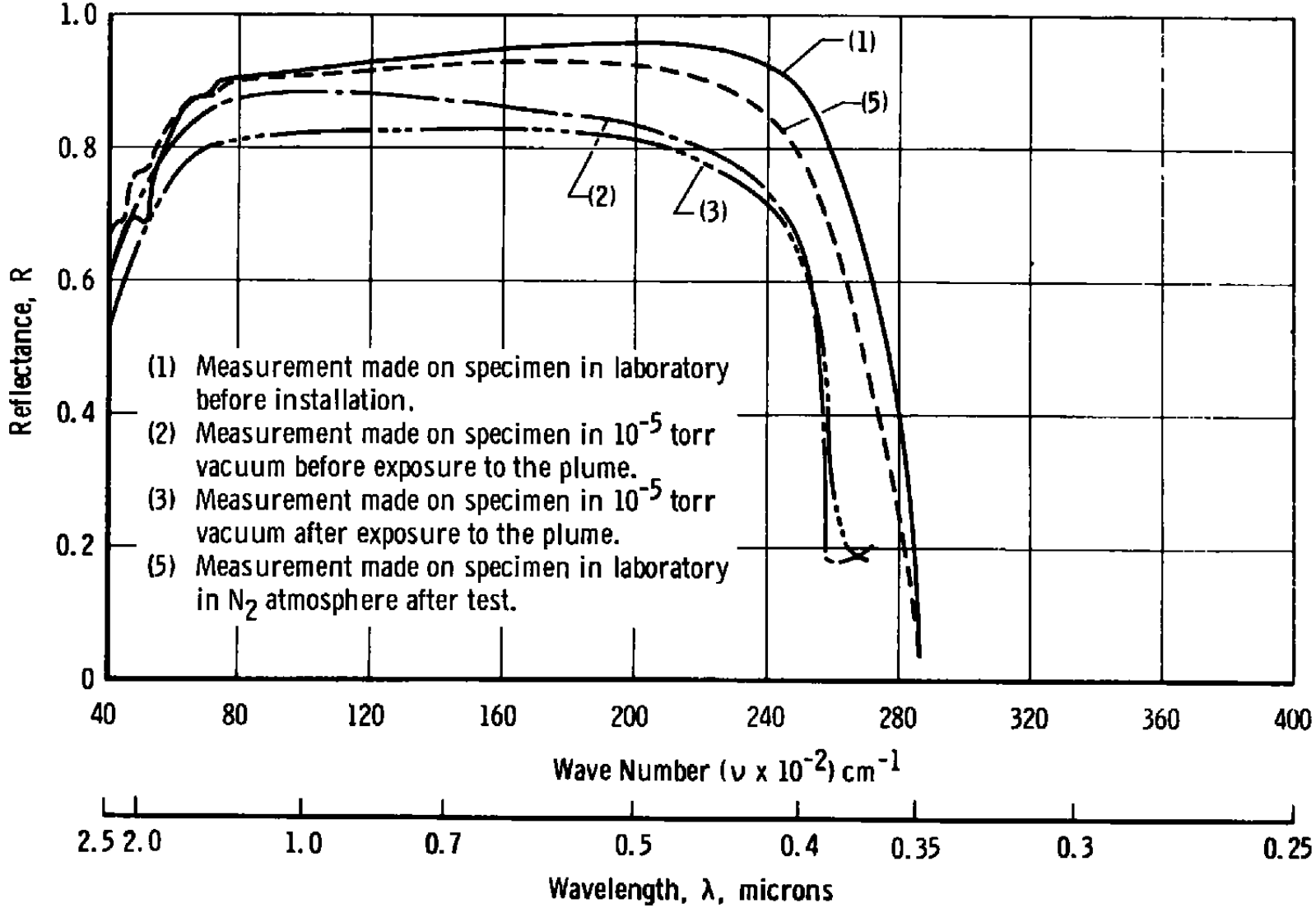

Fig. 38 Test 19—Reflectance Measurements on Specimen, Location S_{19}, Type A

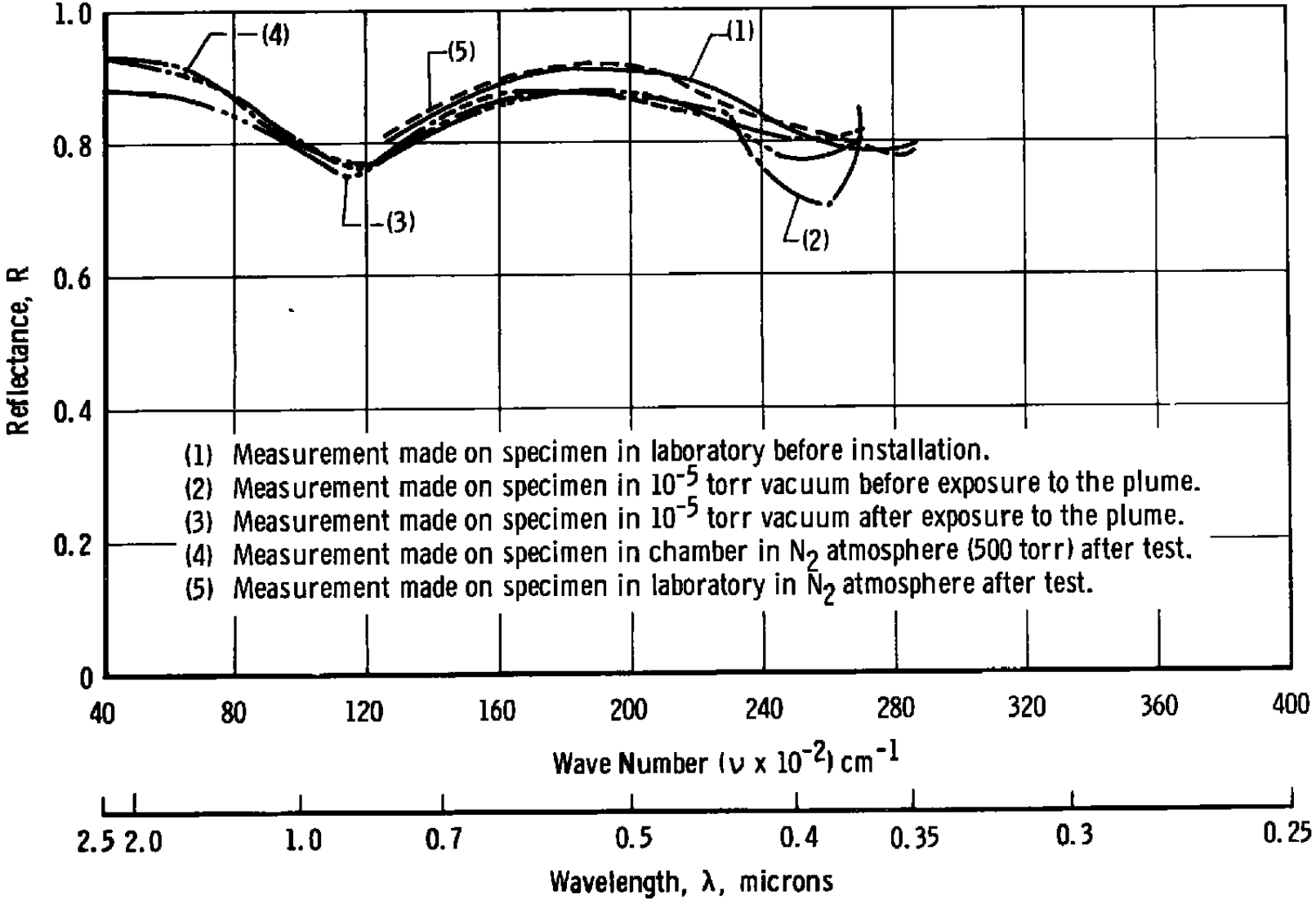

Fig. 39 Test 19—Reflectance Measurements on Specimen, Location S_{24}, Mirror

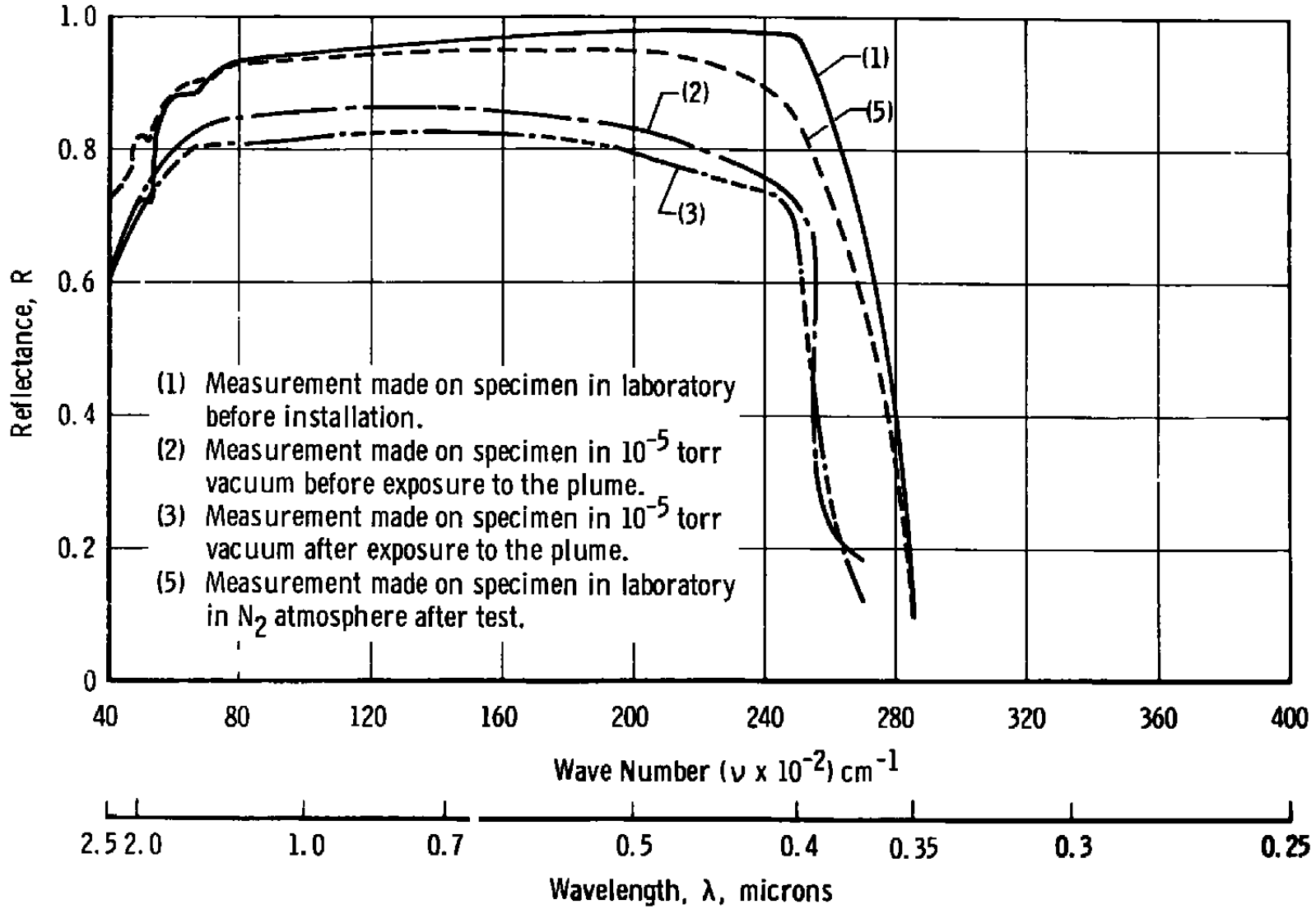

Fig. 40 Test 19—Reflectance Measurements on Specimen, Location S_{28}, Type A

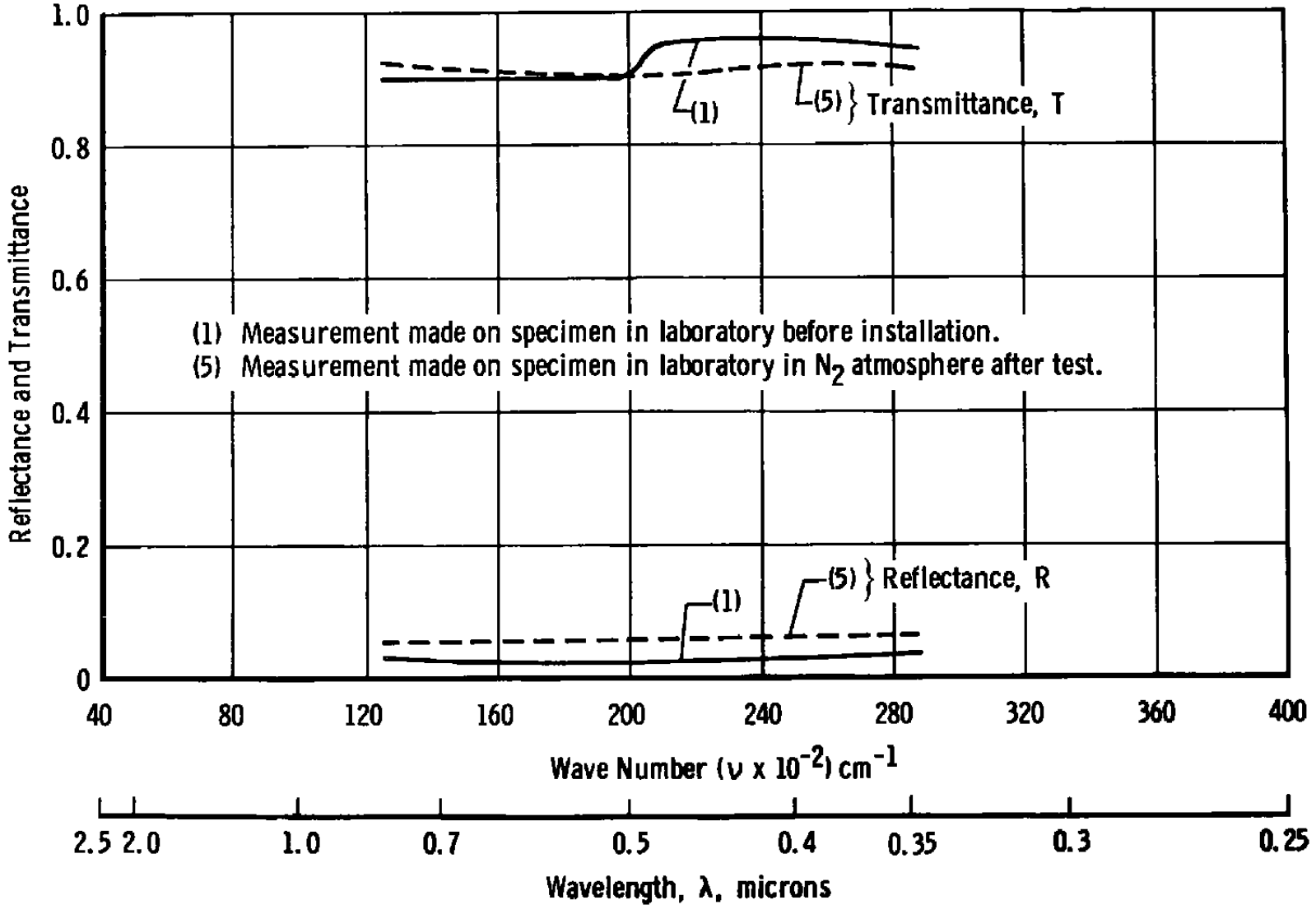

Fig. 41 Test 19--Reflectance and Transmittance Measurements on Specimen, Location S_{27}, Window

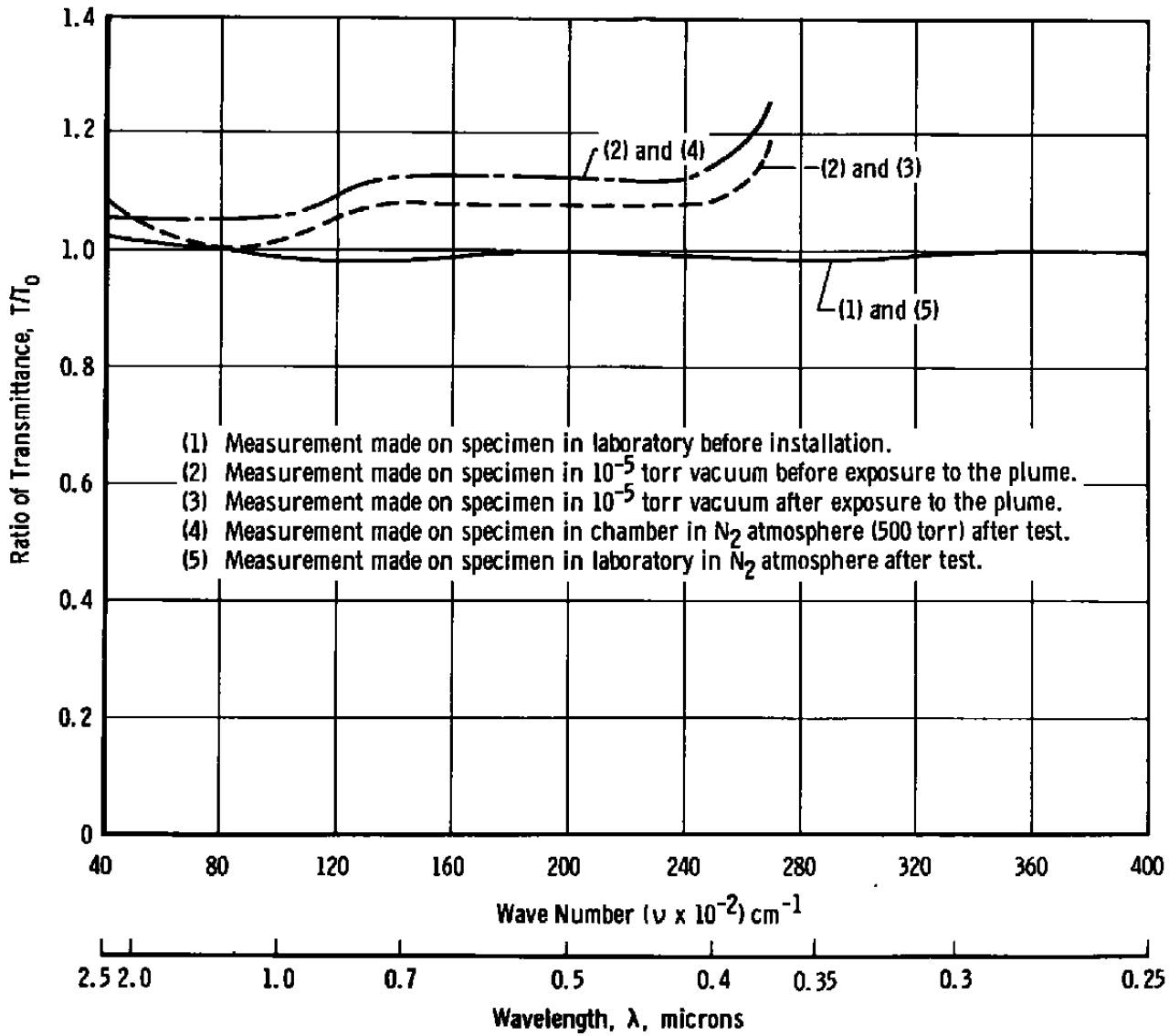

Fig. 42 Test 19—Transmittance Measurements on Specimen, Location V_2, View Port Window

APPENDIX II
TEST LOG

TEST 17

RADIAL THRUSTER (PULSE FIRING)

OBJECTIVE: Determine the amount of contamination from the 1-lb thruster in the radial orientation.

RESULTS: Large amounts of contamination formation on the test panel (Fig. 7). Because of the effect of gravity, contamination flowed down the test panel.

TEST HARDWARE:
Contamination Test Panel 1
View Port Specimen
Horizon Sensor Specimen
Mirror and Window Specimens
Surface Coating Specimens
Velocity Vector Sensor Assembly
4-in. Fence Shielding S23 and S25

TEST CONDITIONS: h = 0.70 in., α = 90 deg, P_{ox} = 150 psia, P_F = 125 psia, Altitude = 400,000 to 600,000 ft

Run No.	Pulsing Mode on (msec) / off (msec) / No. of Pulses	Specimen Measurement Sequence	Photographic Coverage
		Pretest Laboratory	
		Prefire In Situ	
17-1	20/1000/2300		Motion Pictures
17-2	20/1000/700	Postfire In Situ	↓
17-3	50/1000/2400	Postfire In Situ	
17-4	100/1000/1200		
17-5	1000/1000/120		
		Posttest Laboratory	

Test 18

Specimen Location	Type	Pre Lab	In Situ							Post Lab
			Pre	Post	Post	Post	Post	Post	Post S. L.	
S1	VVSA									
S2	A	R								R
S3	A	R								R
S4	A	R								R
S5										
S6	A	R								R
S7	K	R								R
S8										
S9	A	R								R
S10	A	R								R
S11	K	R								R
S12	A	R								R
S13	A	R								R
S14	Emcal									
S15	A	R								R
S16	K									
S17	A	R								R
S18										
S19	A	R								R
S20	K	R								R
S21	A	R								R
S22										
S23	W	T								T
S24	M	R								R
S25	M	R								R
S26	A	R								R
S27	W	T								T
S28	A	R								R
H1	A	R								R
V1										
H2	H									T
V2	V	T								T
G1										
G2										
G3										
G4										
G5										
G6										
G7										
G8										
G9										
G10										
G11										
G12										

TEST 19

RADIAL THRUSTER (PULSE FIRING)

OBJECTIVE: Verify the results of Test 18.

RESULTS: Same as test 18, contamination reduced in panel.

TEST HARDWARE: Contamination Test Panel 1
View Port Specimen
Horizon Sensor Specimen
Mirror and Window Specimens
Surface Coating Specimens
Velocity Vector Sensor Assembly
4-in. Fence Shielding S23 and S25
Shroud and Flask

TEST CONDITIONS: h = 0.70 in., α = 90 deg, P_{ox} = 150 psia, P_F = 125 psia, Altitude = 400,000 to 600,000 ft

Run No.	Pulsing Mode on (msec) / off (msec) / No. of Pulses	Specimen Measurement Sequence	Photographic Coverage
		Pretest Laboratory	
		Prefire In Situ	
Heated shroud to 700°F for all runs.			
19-1	20/1000/523		Motion Pictures
19-2	20/1000/491		
19-3	20/1000/135		
19-4	20/1000/1852	Postfire In Situ	
19-5	50/1000/1538		
19-6	50/1000/130		
19-7	50/1000/732	Postfire In Situ	
19-8	100/1000/1200	Postfire In Situ	
19-9	1000/1000/120	Postfire In Situ	
		Sea-Level In Situ	
		Posttest Laboratory	

Test 17

Specimen Location	Type	Pre Lab	In Situ							Post Lab
			Pre	Post 2	Post 3	Post	Post	Post	Post S. L.	
S1	VVSA									
S2	A	R	R, ε	R, ε	R, ε					R
S3	A	R								R
S4	A	R	R, ε	R, ε						R
S5										
S6	A	R								R
S7	K	R								R
S8	D	R								R
S9	A	R								R
S10	A	R	R, ε	R, ε	R, ε					R
S11	K	R								R
S12	A	R								R
S13	A	R								R
S14	Emcal									
S15	A	R	R, ε	R, ε						R
S16	K	R								R
S17	A	R	R, ε	R, ε						R
S18	D	R								R
S19	A	R	R, ε	R, ε						R
S20	K	R								R
S21	A	R								R
S22										
S23	W	T								T
S24	M	R	R	R						R
S25	M	R								R
S26	A	R								R
S27	W	T								T
S28	A	R	R, ε	R, ε						R
H1	A	R								R
V1										
H2	H									T
V2	V		T	T						T
G1										
G2										
G3										
G4										
G5										
G6										
G7										
G8										
G9										
G10										
G11										
G12										

TEST 18

RADIAL THRUSTER (PULSE FIRING)

OBJECTIVE: Investigate feasibility of heated shroud for capturing and decomposing the contamination generated by thruster, therefore reducing amount of deposited on panel.

RESULTS: The heated shroud reduced significantly the amount of contamination on the panel that previously had been observed.

TEST HARDWARE: Contamination Test Panel 1
View Port Specimen
Horizon Sensor Specimen
Mirror and Window Specimens
Surface Coating Specimens
Velocity Vector Sensor Assembly
Shroud with Tube to Vacuum Container

TEST CONDITIONS: h = 0.70 in., α = 90 deg, P_{ox} = 150 psia,
P_F = 125 psia, Altitude = 400,000 to 600,000 ft

Run No.	Pulsing Mode on / off / No. of (msec) / (msec) / Pulses	Specimen Measurement Sequence	Photographic Coverage
		Pretest Laboratory	
Heated shroud to 200°F for all runs.			
18-1	20/1000/301		Motion Pictures
18-2	20/1000/2130		↓
18-3	20/1000/569		
18-4	50/1000/164		
18-5	50/1000/736		
18-6	50/1000/1500		
18-7	100/1000/1200		
18-8	1000/1000/120		
		Posttest Laboratory	

Test 19

Specimen Location	Type	Pre Lab	In S.tu							Post Lab
			Pre	Post 4	Post 7	Post 8	Post 9	Post	Post S. L.	
S1	VVSA									
S2	A	R	R, ε	R, ε	R, ε	R, ε	R, ε		R	R
S3	A	R								R
S4	A	R	R, ε	R, ε	R, ε	R, ε	R, ε		R	R
S5										
S6	A	R								R
S7	K	R								R
S8										
S9	A	R								R
S10	A	R	R, ε	R, ε	R, ε	R, ε	R, ε		R	R
S11	K	R								R
S12	A	R								R
S13	A	R								R
S14	Emcal									
S15	A	R	R, ε	R, ε	R, ε	R, ε	R, ε		R	R
S16	K	R								R
S17	A	R	R, ε	R, ε	R, ε	R, ε	R, ε		R	R
S18										
S19	A	R	R, ε	R, ε	R, ε	R, ε	R, ε		R	R
S20	K	R								R
S21	A	R								R
S22										
S23	W									
S24	M	R	R	R	R	R	R		R	R
S25	M									
S26	A	R								R
S27	W	T								T
S28	A	R	R, ε	R, ε	R, ε	R, ε	R, ε		R	R
H1	A	R								R
V1										
H2	H									T
V2	V	T	T	T	T	T	T		T	T
G1										
G2										
G3										
G4										
G5										
G6										
G7										
G8										
G9										
G10										
G11										
G12										

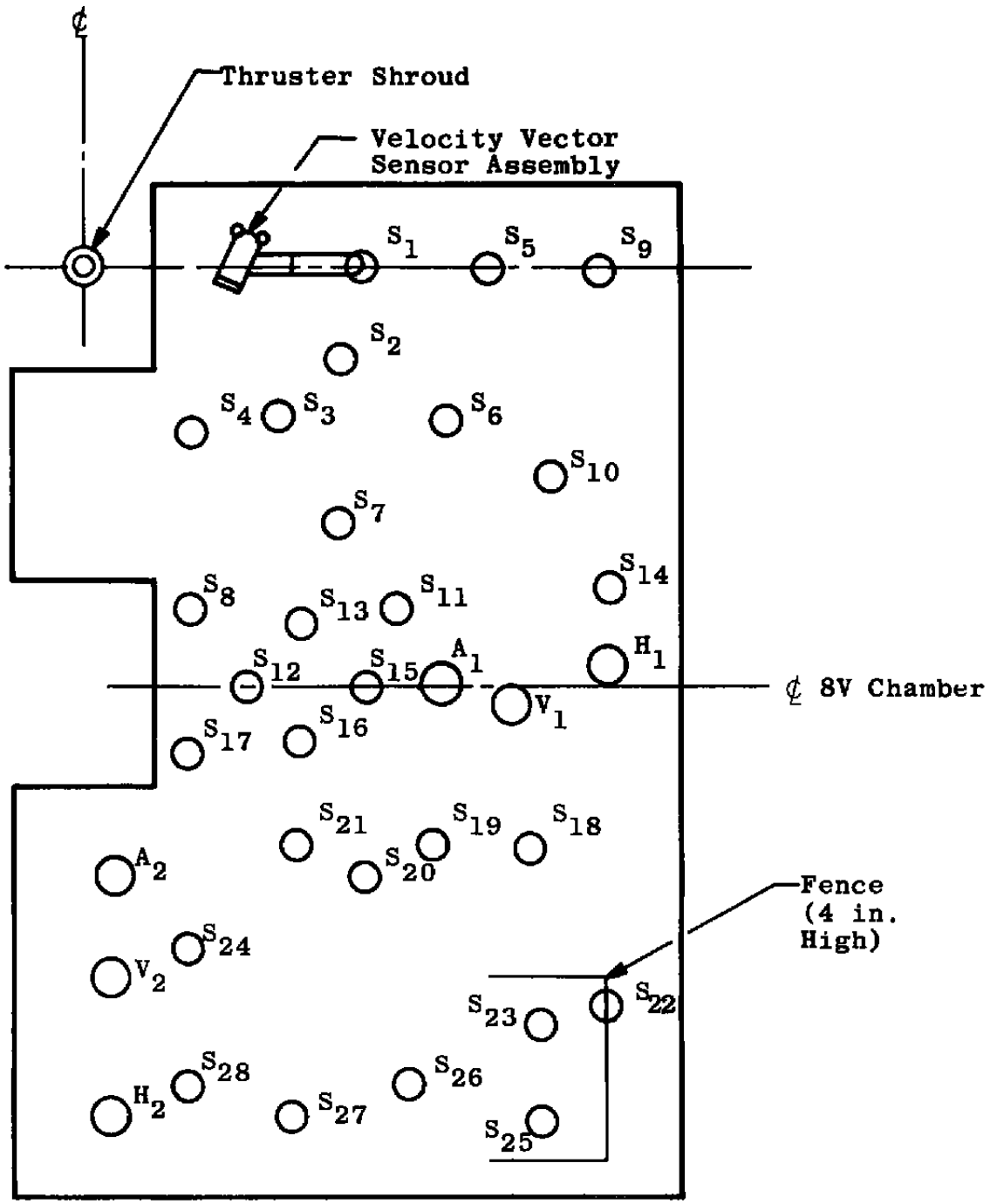

Fig. II-1 Contamination Controls on Thruster and Panel Used during Radial Tests

APPENDIX III
TABLES OF OPTICAL MEASUREMENTS

TABLE 1

Primary Test 17

Firing No.	Solar Absorptance, α_s	Emittance, ϵ	α_s/ϵ	Average Visible Reflectance, $\bar{R}$	Specimen Location and Type
0	0.2141	0.9807		0.7216	S2A
2	0.1468	0.9826		0.7721	S2A
3		0.9733			S2A
0	0.3214	0.9749		0.8592	S4A
2	0.1633	0.9785		0.7724	S4A
0	0.1884	0.9667		0.7453	S10A
2	0.1607	0.9615		0.7790	S10A
3		0.9643			S10A
0	0.4802	0.9332		0.5554	S15A
2	0.3542	0.9634		0.6784	S15A
0	0.1679	0.9816		0.7674	S17A
2	0.1694	0.9744		0.7810	S17A
0	0.2158	0.9925		0.6927	S19A
2	0.2118	0.9943		0.7048	S19A
0	0.2230	0.9929		0.7044	S28A
2	0.2465	0.9880		0.6899	S28A
0	0.1664			0.8226	S24M
2	0.1479			0.8506	S24M
	Solar Transmittance			Average Visible Transmittance	
0					V2
2	0.9828			0.9787	V2

TABLE 11

Primary Test 19

Firing No.	Solar Absorptance, α_s	Emittance, ϵ	α_s/ϵ	Average Visible Reflectance, $\bar{R}$	Specimen Location and Type
0	0.1664	0.9823		0.7679	S2A
4	0.1697	0.9742		0.7623	S2A
7	0.2802	0.9717		0.6993	S2A
8	0.2062	0.9773		0.7375	S2A
9	0.2070	0.9859		0.7424	S2A
S.L.	0.1939			0.7388	S2A
0	0.1683	1.026		0.7683	S4A
4	0.1688	1.145		0.7669	S4A
7	0.2878	0.9846		0.6964	S4A
8	0.3926	0.9969		0.6135	S4A
9		0.9894			S4A
S.L.	0.1938			0.7453	S4A
0	0.1652	0.9701		0.7720	S10A
4	0.2309	0.9685		0.6878	S10A
7	0.1054	0.9696		0.8378	S10A
8	0.2445	0.9809		0.7324	S10A
9		0.9528			S10A
S.L.	0.2016			0.7500	S10A
0	0.1627	0.9732		0.7762	S15A
4	0.1683	0.9696		0.7685	S15A
7	0.2056	0.9739		0.7367	S15A
8		0.9642			S15A
9	0.2064	0.9821		0.7362	S15A
S.L.	0.1974			0.7446	S15A

TABLE 11 (Con't)

Primary Test 19

Firing No.	Solar Absorptance, α_S	Emittance, ϵ	α_S/ϵ	Average Visible Reflectance, $\bar{R}$	Specimen Location and Type
0	0.1664	0.9805		0.7785	S17A
4	0.1784	0.9666		0.7581	S17A
7	0.2306	0.9849		0.7075	S17A
8	0.2037	0.9662		0.7397	S17A
9	0.2178	0.9875		0.7305	S17A
S.L.	0.1919			0.7626	S17A
0	0.1674	0.9836		0.7621	S19A
4	0.1643	0.9942		0.7692	S19A
7	0.2235	0.9903		0.7156	S19A
8	0.2163	0.9944		0.7190	S19A
9	0.2124	0.9915		0.7300	S19A
S.L.	0.1993			0.7384	S19A
0	0.1873	0.9557		0.7490	S28A
4	0.1885	0.9518		0.7496	S28A
7	0.2646	0.8880		0.7083	S28A
8	0.2114	0.9636		0.7205	S28A
9	0.2009	0.9668		0.7445	S28A
S.L.					S28A
0	0.1558			0.8345	S24M
4					S24M
7					S24M
8	0.1725			0.8270	S24M
9	0.1607			0.8297	S24M
S.L.	0.1549			0.8520	S24M

TABLE 11 (Concluded)

Primary Test 19

Firing No.	Relative Solar Transmittance, t_s	Average Visible Relative Transmittance, $\overline{T}$	Specimen Location and Type
0			V2
4			V2
7	0.074	1.085	V2
8	1.061	1.079	V2
9			V2
S.L.	1.093	1.136	V2

UNCLASSIFIED
Security Classification

DOCUMENT CONTROL DATA - R & D

(Security classification of title, body of abstract and indexing annotation must be entered when the overall report is classified)

1. ORIGINATING ACTIVITY (Corporate author)	2a. REPORT SECURITY CLASSIFICATION
Arnold Engineering Development Center ARO, Inc., Operating Contractor Arnold Air Force Station, Tennessee	UNCLASSIFIED
	2b. GROUP N/A

3 REPORT TITLE

EFFECTS AND CONTROL OF CONTAMINATION FROM A SCALED MOL ATTITUDE CONTROL THRUSTER IN A RADIAL ORIENTATION

4 DESCRIPTIVE NOTES (Type of report and inclusive dates)

May through December 21, 1968 - Final Report

5 AUTHOR(S) (First name, middle initial, last name)

David W. Hill, Jr. and Dale K. Smith, ARO, Inc.

6. REPORT DATE	7a. TOTAL NO OF PAGES	7b. NO OF REFS
October 1969	78	13

8a. CONTRACT OR GRANT NO.	9a. ORIGINATOR'S REPORT NUMBER(S)
F40600-69-C-0001	
b. Program Element 35121F	AEDC-TR-69-175
c. Program Area 632A	9b. OTHER REPORT NO(S) (Any other numbers that may be assigned this report)
d.	N/A

10. DISTRIBUTION STATEMENT This document may be further distributed by any holder only with specific prior approval of MOL Project Office (SAFSL-5B), AF Unit Post Office, Los Angeles, California 90045.

11. SUPPLEMENTARY NOTES	12. SPONSORING MILITARY ACTIVITY
Available in DDC	MOL Project Office (SAFSL-3) AF Unit Post Office Los Angeles, California 90045

13. ABSTRACT

A test was conducted to determine the effects of contamination produced by a 1-lb scaled Manned Orbital Laboratory thruster. The test required pulsing the 1-lb attitude control thruster in its radial orientation and determining the effects of contaminates from the thruster impinging on optical and thermal control surface test specimens located on a flat plate exposed to the thruster exhaust plume. The thruster was pulsed with durations of 20, 50, 100, and 1000 msec with 1000 msec off time at altitudes above 400,000 ft. Significant contamination was produced for the pulse-mode operation. Methods for control of contamination from the thruster and on the plate were investigated. In situ reflectance, emittance, and transmittance measurements were made on the optical and thermal control surface test specimens under vacuum conditions and at atmospheric pressure. Pretest and posttest laboratory measurements were made at atmospheric conditions. Contamination deposited on the plate was near and below the thruster exit, and the amount of contamination produced by the thruster decreased as the thruster pulse duration increased. Contamination controls evaluated during the test were the heated shroud and a fence located on the plate. The heated shroud was effective in reducing contamination on the plate; however, it did not eliminate the contaminates produced by the thruster in the plume. The in situ reflectance and transmittance measurements made on the specimens at the simulated altitude were more realistic of the contamination encountered by the specimens from the thruster exhaust than the atmospherical posttest laboratory measurements.

This document may be further distributed by any holder only with specific prior approval of MOL Project Office (SAFSL-5B), AF Unit Post Office, Los Angeles, California 90045.

DD FORM 1 NOV 68 1473

UNCLASSIFIED
Security Classification

14. KEY WORDS	LINK A		LINK B		LINK C	
	ROLE	WT	ROLE	WT	ROLE	WT
Manned Orbital Laboratory						
thrusters						
contamination						
control						
steady state						
pulse spacing modulation						
reflectance						
emittance						
transmittance						

AFSC
Arnold AFS Tenn